Photochemistry and Photophysics of Triarylmethane Dye Leuconitriles

Viktor V. Jarikov and Douglas C. Neckers*

Center for Photochemical Sciences,[1] Bowling Green State University, Bowling Green, Ohio 43403

neckers@photo.bgsu.edu

The photochemical reactions of crystal violet leuconitrile (CVCN) were investigated by the means of product analysis and trapping experiments, laser flash and steady-state photolysis, and steady-state fluorescence. The influence of oxygen on the reaction was examined in detail. The photochemistry of malachite green leuconitrile (MGCN), basic fuchsin leuconitrile (BFCN), and crystal violet leucomethyl (CVMe) and leucobenzyl (CVBn), as well as triphenylacetonitrile, was studied. The results suggest ionization occurs from S_1, while the di-π-methane reaction is the photochemical route from T_1.
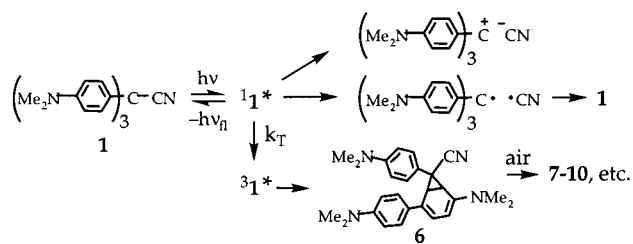
Introduction

The photodissociation of compounds of the polyaryl-methyl-X series, the excited precursors, the primary products, and the secondary reactions have been a topic of intense interest and dispute.[2–8] Depending on the structure and the solvent, either bond homolysis, bond heterolysis, or both occur.[2,3,9–13] The photogeneration of carbocations[7,11,14–16] and the photochromism of triarylmethane (TAM) leuco dyes[17–20] have been reviewed. The compounds have been of particular interest as sources of instantaneous color. The photoinduced dissociation of a triarylmethane dye leuconitrile (TAM-CN) to form the dye cation (TAM⁺) was first observed in 1900[21] though not really discovered until 1919.[22] The quantum yields of dye and cyanide anion[23] formation from CVCN and

MGCN have been reported to vary from 0.9 to 1.0 in ethanol and from 0.65 to 0.96 in acetonitrile.[24–26] Holmes showed that heterolysis is more efficient in more polar solvents,[27] though water remains an unexplained anomaly.[25,28] Herz demonstrated that S_1 was the precursor of ionization.[29] Their findings have been confirmed.[7,25,26,30] On the basis of the biexponential rise of the transient absorption, Cremers and Cremers suggested TAM-CNs produce TAM⁺ initially in a pyramidal geometry, which then relaxes into the planar conformation.[31] However, Manring and Peters determined the short component to be due to S_1.[32] Spears et al. found the long component matched the kinetics of fluorescence decay, which established MG⁺ was created directly from S_1.[26] The short part of the absorption rise was absent in the fluorescence decay kinetics and assigned to the tetrahedral ion pair. Miller et al. measured the photoionization rate constants (10^{10}–10^7 s⁻¹) as a function of temperature and found the activation energy low (~1 kcal/mol) in various solvents.[33] They concluded that favorable changes in solvent entropy are necessary to achieve the partially charged molecular geometry that leads to barrierless ionization.

Repeated photochromic cycling of a TAM-CN leads to the yellow "colorless" state and reduces the efficiency of coloration.[14,24] Moreover, the chromophore is destroyed by irradiation in nonpolar solvents.[27] An unusually low value of 0.75 for the MGCN actinometer[34] and formation of an unknown absorption band at 350 nm were also reported.[35] Holmes and others[2,8,36] attributed these ob-

(1) Contribution no. 428 from the Center for Photochemical Sciences.
(2) Bartl, J.; Steenken, S.; Mayr, H.; McClelland, R. A. *J. Am. Chem. Soc.* **1990**, *112*, 6918.
(3) Pohlers, G.; Scaiano, J. C.; Step, E.; Sinta, R. *J. Am. Chem. Soc.* **1999**, *121*, 6167.
(4) Siskos, M. G.; Zarkadis, A. K.; Steenken, S.; Karakostas, N. *J. Org. Chem.* **1999**, *64*, 1925.
(5) Faria, J. L.; Steenken, S. *J. Phys. Chem.* **1993**, *97*, 1924.
(6) Dreyer, J.; Peters, K. S. *J. Phys. Chem.* **1996**, *100*, 15156.
(7) Cristol, S. H.; Bindel, T. H. *Org. Photochem.* **1983**, *6*, 327.
(8) Minto, R. E.; Das, P. K. *J. Am. Chem. Soc.* **1989**, *111*, 8858.
(9) McClelland, R. A.; Kanagasabapathy, V. M.; Banait, N. S.; Steenken, S. *J. Am. Chem. Soc.* **1989**, *111*, 3966.
(10) Ivanov, V. B.; Ivanov, V. L.; Kuz'min, M. G. *Mol. Photochem.* **1974**, *6*, 125.
(11) Das, P. K. *Chem. Rev.* **1993**, *93*, 119.
(12) Kropp, P. J. *Acc. Chem. Res.* **1984**, *17*, 131.
(13) Kaneko, Y.; Neckers, D. C. *J. Phys. Chem. A* **1998**, *102*, 5356.
(14) Bertelson, R. C. In *Photochromism*; Brown, G. H., Ed.; Techniques of Chemistry; Wiley-Interscience: New York, 1971; Vol. 3, Chapters 3 and 10.
(15) Boyd, M. K. In *Organic Photochemistry*; Ramamurthy, V., Shanze, K. S., Eds.; Dekker: New York, 1997; p 147.
(16) McClelland, R. A. *Tetrahedron* **1996**, *52*, 6823.
(17) Kosar, J. *Light Sensitive Systems. Chemistry and Applications of Nonsilver Halide Photographic Processes*; Wiley: New York, 1965; Chapter 8, p 358.
(18) Duxbury, D. F. *Chem. Rev.* **1993**, *93*, 381.
(19) Muthayala, R. In *Chemistry and Applications of Leuco Dyes*; Katritzky, A. R., Sabongi, G. J., Eds.; Topics in Applied Chemistry; Plenum Press: New York, 1997.
(20) Arnett, E. M.; Flowers, R. A.; Ludwig, R. T.; Meekhof, A. E.; Walek, S. A. *J. Phys. Org. Chem.* **1997**, *10*, 499.
(21) Hantzsch, Ă.; Osswald, G. *Chem. Ber.* **1900**, *33*, 306.
(22) Lifschitz, J. *Ber.* **1919**, *52*, 1919; *Chem. Abstr.* **1920**, *14*, 1984.

(23) Szychlinski, J. *Rocz. Chem.* **1967**, *41*, 2123.
(24) Dessauer, R.; Paris, J. P. *Adv. Photochem.* **1963**, *1*, 275.
(25) Geiger, M. W.; Turro, N. J.; Waddell, W. H. *Photochem. Photobiol.* **1977**, *25*, 15.
(26) Spears, K. G.; Gray, T. H.; Huang, D. *J. Phys. Chem.* **1986**, *90*, 779.
(27) Holmes, E. O., Jr. *J. Phys. Chem.* **1966**, *70*, 1037.
(28) Sporer, A. H. *Trans. Faraday Soc.* **1961**, *57*, 983.
(29) Herz, M. L. *J. Am. Chem. Soc.* **1975**, *97*, 6777.
(30) Brown, F. G.; Cosa, J. *Chem. Phys. Lett.* **1977**, *45*, 429.
(31) Cremers, D. A.; Cremers, T. L. *Chem. Phys. Lett.* **1983**, *94*, 102.
(32) Manring, L. E.; Peters, K. S. *J. Phys. Chem.* **1984**, *88*, 3516.
(33) Miller, R. M.; Spears, K. G.; Gong, J. H.; Wach, M. *J. Phys. Chem.* **1994**, *98*, 1376.
(34) Kemula, W.; Grabowska, A. *Rocz. Chem.* **1960**, *34*, 1445.
(35) Germann, F. E. E.; Gibson, C. L. *J. Am. Chem. Soc.* **1940**, *62*, 110.

Scheme 1. Photochemistry of CVCN

Figure 1. (A) UV absorption spectrum of CV^+Cl^- in aceto-nitrile ($+HCl$, average of 4, $\epsilon^{306} = 26800$ and $\epsilon^{588} = 112200$ $M^{-1}\ cm^{-1}$); (B) UV absorption and normalized fluorescence spectra of **1**.

servations to homolysis of the C−CN bond.[27] Although never shown directly, this has been widely supported[17] and, for example, used to explain the degradation of TAM leuco dyes in various polymers.[37] In support of this suggestion, 9-phenylxanthen-9-ol preferentially produces the xanthyl radical in *n*-heptane, mainly the cation in polar solvents, and both species in acetonitrile.[8] McClelland and co-workers found that heterolysis depends on the nature of *para*-substituents in Ar_2CHX, while homolysis is not similarly influenced. Preferential formation of the radical over the cation was observed, and the yield of both species increased in more polar solvents.[2,9,38] Typically, sensitization of the process led to a higher yield of radicals.[3] The so-called "*meta* electron transmission effect" on heterolysis was rationalized by Zimmerman[39] and confirmed.[7] However, Pincock questioned this interpretation instead suggesting that electron transfer (e^-T) follows initial homolysis and forms the products of heterolysis.[40] On the other hand, Peters and co-workers showed both the cation and the radical were produced directly from S_1 of Ph_2CHCl in <20 ps.[41] Also, they noticed that the electron affinity of the leaving group controls homolysis in nonpolar solvents and concluded that heterolysis is followed by e^-T to give radicals in <25 ps.[32] In contrast, Bartl et al. suggested that heterolysis and homolysis for the halides are in direct competition.[2] Siskos et al. showed that homolysis in *N*-(trityl)anilines is independent of solvent, and the yield of radicals increases drastically in the series $PhCH_2NHPh$, $Ph_2-CHNHPh$, and Ph_3CNHPh.[4] Similar results were obtained in studies of methoxybenzyl, -benzhydryl, and -trityl acetates, but dissociation originated from T_1, as opposed to S_1 in the case of benzyl, naphthylmethyl, and anthrylmethyl acetates.[10]

Sporer,[28] supported by others,[14,25,29] found that N−Me cleavage ($\phi = 0.02$) occurs in TAM-CNs in lieu of C−CN cleavage. Herz suggested that destruction of the TAM chromophore occurs through photodegradation of TAM^+.[29] However, there are no intramolecular photoreactions of CV and MG-type dyes known that destroy them efficiently in dilute solutions.[15,18] Shi et al. proposed α,α-elimination (di-π-methane reaction) in $^1TAM-X^*$ forms a biaryl and a carbene ($\phi = 0.01-0.05$).[42] An analogous elimination has been reported for triptycene,[43] Ar_3P,[44]

Ar_3Al,[45] and Ar_3B.[46] For TAM amines, ketones, phosphonates, and cyanides, α,α-elimination competes with homolysis of the C−X bond ($\phi = 0.06$, X = CN).[47]

To the best of our knowledge, the fate of $^3TAM-CN^*$ has not been investigated although there is the wealth of information about the nature of S_1. Our data indicate $^3TAM-CN^*$ undergoes the di-π-methane rearrangement (DPMR),[48] which leads to yellow products and transformation of the chromophoric system. We have shown that this reaction occurs with CVCN, MGCN, BFCN, CVMe, CVBn, and it possibly even occurs in the case of trityl cyanide. Also, we suggest homolysis of the C−CN bond takes place in S_1 but is followed by a rapid in-cage recombination of a singlet radical pair (Scheme 1).

Results and Discussion

I. CVCN. Spectral Characteristics. The UV spectrum of CVCN (**1**) resembles the spectrum of *N,N*-dimethylaniline (DMA) or *N,N*-dimethyl-*p*-toluidine (DMT, Figure 1B). It is red-shifted possibly due to weak resonance interaction between the aniline rings.[49] Fluorescence and intersystem crossing (isc) account for the S_1 decay of dialkylanilines, and they are good models for the S_1 of TAM-CNs in nonpolar solvents.[25,30,33] The fluorescence emission spectrum of **1** is characteristic of the $S_1(\pi\pi^*)$ state of DMA/DMT. The fluorescence quantum yield (ϕ_{fl}) decreases with increasing solvent polarity (Table 1), while the efficiency of coloration increases. This is typical for TAM-CNs, and we suggest $^1\mathbf{1}^*$ undergoes an ionization. Computed rate constants and quantum yields of ionization, k_i and ϕ_i, agree well with those reported for MGCN (Table 1).[26] The case with halocarbon solvents is outside of this trend and is attributed to the known oxidation of $\mathbf{1}^*$ by these solvents.[14] The phosphorescence emission of **1** is characteristic of the $T_1(\pi\pi^*)$ state of the aniline/toluidine moiety (Table 2).[29] For MGCN, the quantum yield for T_1 formation (ϕ_T) and isc rate constant (k_T) were determined to be 0.7−0.9 and 2.9 $\times\ 10^8\ s^{-1}$ at room temperature in nonpolar solvents ($\phi_T^{DMA} = 0.9$).[26,50,51] It appears reasonable to take the values of ϕ_T and k_T determined for MGCN as first

(36) Pak, M. A.; Shigorin, D. N.; Ozerova, G. *Dokl. Acad. Nauk SSSR, Phys. Ser.* **1969**, *186*, 311 (English Transl).

(37) Kawai, H.; Nagamura, T. *Photochem. Photobiol. A: Chem.* **1995**, *92*, 105.

(38) Steenken, S.; McClelland, R. A. *J. Am. Chem. Soc.* **1989**, *111*, 4967.

(39) Zimmerman, H. E. *J. Am. Chem. Soc.* **1995**, *117*, 8988.

(40) Pincock, J. A. *Acc. Chem. Res.* **1997**, *30*, 43.

(41) Peters, K. S.; Li, B. *J. Phys. Chem.* **1994**, *98*, 401.

(42) Okamoto, Y.; Shi, M.; Takamuku, S. *J. Synth. Org. Chem. Jpn.* **1992**, *50*, 798, and references therein.

(43) Ipaktshi, J. *Chem. Ber.* **1989**, *105*, 1972.

(44) Changenet, P.; Plaza, P.; Martin, M. M.; Meyer, Y. H.; Rettig, W. *J. Chim. Phys. Phys.-Chem. Biol.* **1996**, *93*, 1697.
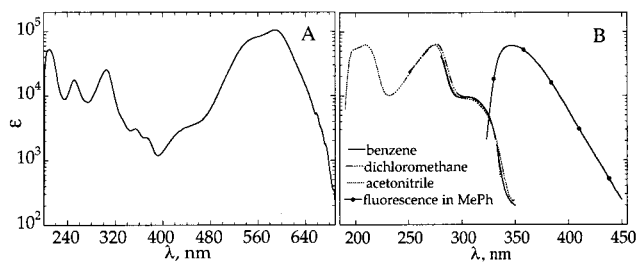
(45) Meinwald, J.; Knapp, S.; Obendorf, S. K.; Hughes, R. E. *J. Am. Chem. Soc.* **1976**, *98*, 6643.

(46) Chalhoun, G. C.; Schuster, G. B. *J. Org. Chem.* **1984**, *49*, 1295.

(47) Shi, M.; Okamoto, Y.; Takamuku, S. *J. Chem. Res.-S* **1990**, 131.

(48) Zimmerman, H. E. In *Rearrangements in Ground and Excited States*; de Mayo, P., Ed.; Academic Press: New York, 1980; Vol. 3, p 131.

(49) Kasha, M.; Rawls, H.; El-Bayoumi, M. In *Proceedings of the Eighth European Congress on Molecular Spectroscopy*; Butterworths: London, 1965; p 371.

(50) Darmanyan, A. P.; Lee, W.; Jenks, W. S. *J. Phys. Chem. A* **1999**, *103*, 2705.

Table 1. Absorption and Fluorescence Maxima and Quantum Yields, Rate Constants and Quantum Yields of Photoionization of 1 and DMA

compd	solvent	$\lambda_{abs}^{max\ g}$	$\lambda_{fl}^{max\ f,e}$	ϕ_{fl}^{c}	k_i, s^{-1}	ϕ_i
DMA	C_6H_{14}	252, 299	331.5	0.11^{j}	-	-
CVCN	C_6H_{14}	270, 304	338	0.07	0	0
CVCN	MePh	306 $(9.6)^{a}$	346	0.08	0	0
CVCN	Et_2O	273, 307	348	0.09	0	0
CVCN	DME^{h}	272, $310s^{b}$	353	0.045	5×10^{8}	0.55
CVCN	$CHCl_3$	275, 310s	357	3×10^{-4}	-	1.0^{d}
CVCN	CH_2Cl_2	275 $(64.3)^{a}$ 310s $(9.2)^{a}$	354	7×10^{-4}	-	1.0^{d}
CVCN	CH_3CN	274 $(62.1)^{a}$ 310s $(8.7)^{a}$	358.5	0.011	3.5×10^{9}	0.89
CVCN	MeOH	272, 310s	356	4×10^{-3}	9×10^{9}	0.96

^{a} $\epsilon \times 10^{-3}$, M^{-1} cm^{-1}, averaged. ^{b} Shoulder. ^{c} In the aerated solutions ϕ_{fl}'s were slightly lower. ^{d} $\phi_{CV^{+}}$ = observed yield of CV^{+}. ^{e} 365 nm in acetone. ^{f} Emission maximum, nm. ^{g} Ground-state absorption maxima, nm. ^{h} 1,2-dimethoxyethane. ^{j} Reference 51.

Table 2. Photophysical Parameters of 1

E_S, PhH/EtOH, kJ/mol^{b,d}	370/360
τ_S, PhH/MeOH, ns^{c}	2.5/0.1
E_T, 1^{c}/DMA,^{e} kJ/mol	310/320
τ_T, 77 K, PhH^{f}/rt, Et_2O,^{b} μs	1.5×10^{5}/0.18
ϕ_T, n/p,^{a,c} rt/ϕ_{ph}, n/p,^{a,f} 77 K	0.8/0.03 / 0.3/0.3
k_{fl}, $s^{-1\ c}$/k_T, $s^{-1\ c}$	3.8×10^{7}/3.2×10^{8}

^{a} In nonpolar/polar solvent. ^{b} Determined in this study. ^{c} For MGCN, refs 26, 33 (see text). ^{d} Calculated from λ^{0-0}. ^{e} Reference 51. ^{f} Reference 29.

approximations to the corresponding values for **1** (Table 2). Note the ionization reaction does not occur from T_1.[27−29,31,33]

Steady-State Photolysis. (a) UV−vis. Upon 300-nm irradiation under argon or air, **1** gave rise to CV^{+} in solvents with $\epsilon \geq \sim5$ (Figure 1A). In degassed solvents with $\epsilon < \sim30−35$, a new 320−400 nm "yellow" absorption band ($\lambda_{max} \sim 370$ nm) was produced. The yellow band was absent in aerated solutions. The changes observed in the 200−400 nm range in degassed hexanes indicate three distinct steps in this photolysis. On the basis of the structures of final products **7−10** isolated in product studies, we suggest norcaradiene **6** ($\lambda_{max} \sim 370$ nm, Scheme 2) is formed in the first step. The growth of the 370-nm band is concomitant with the decrease of the absorption by **1** at 210 and 270 nm. In the second step, the 370-nm band decays due to photochemical reactions of **6**, and a 305-nm band grows. Further irradiation leads to the decrease of absorbance throughout the whole spectral region and may be attributed to decomposition. The yellow band continued to grow in the dark (k $\sim 5 \times 10^{-4}$ s^{-1} at 20 °C, faster at 80 °C). This "dark reaction" may be norcaradiene **4** undergoing C[1,5] migration to afford a conjugated valence tautomer, norcaradiene **6** (Scheme 2). The yellow band, **6**, decayed very slowly in the dark under argon (k $\sim 1 \times 10^{-6}$ s^{-1} at 20 °C, 2 $\times 10^{-3}$ at 80 °C, and very fast under 350-nm irradiation) into a species that has no absorption above 320 nm, presumably its valence tautomer diarylacetonitrile **7** (Scheme 2). Carbon migrations in norcaradienes and their conversion to toluenes are known and common.[52] Exposure of irradiated samples to air caused the yellow solutions to slowly turn brown-black due to the "post-irradiation oxidation reaction" (PIOR).

(51) Murov, S. L.; Carmichael, I.; Hug, G. L. *Handbook of Photochemistry*; Dekker: New York, 1993.

(52) Jarzecki, A. A.; Gajewski, J.; Davidson, E. R. *J. Am. Chem. Soc.* **1999**, *121*, 6928.

Scheme 2. Irradiation of CV−R in Degassed Benzene: Di-π-methane Reaction → C[1,5] Migration → Thermal and Photochemistry of Norcaradiene 6x (CVCN: R = CN, x = −; CVMe: R = Me, x = a; CVBn: R = Bn, x = b)
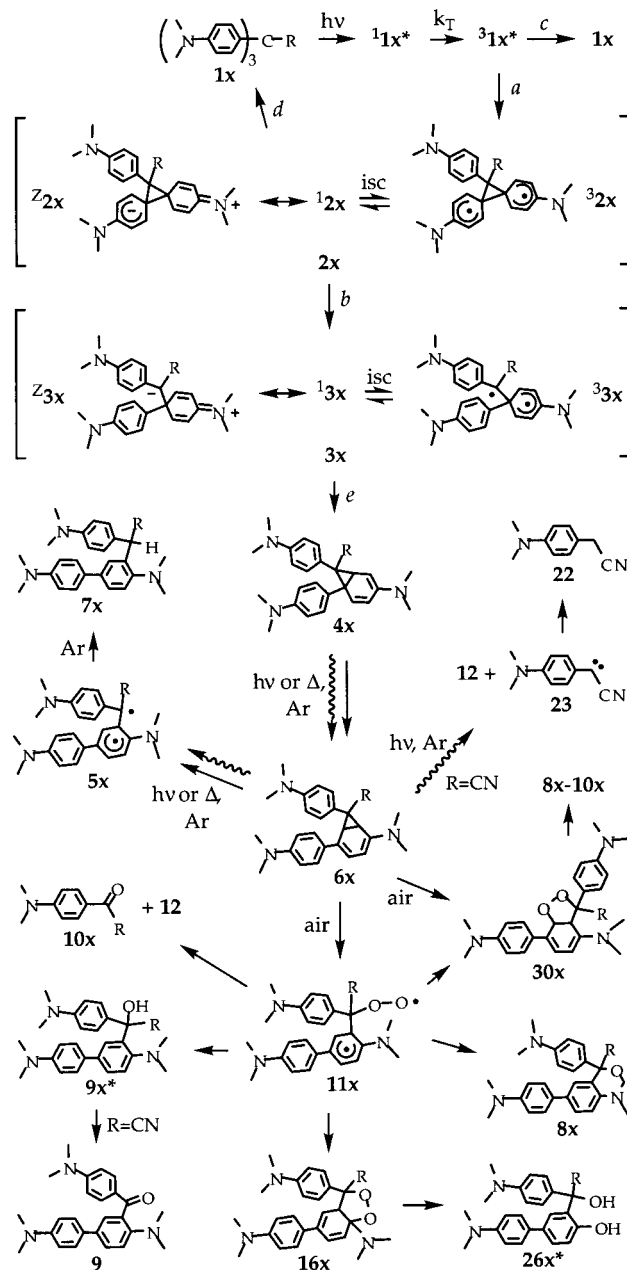
(b) NMR. Samples were irradiated in degassed C_6D_6 with the 300-nm light. Using benzophenone−benzhydrol actinometry the I_0 for a Pyrex NMR tube was found to be about 4×10^{21} quanta L^{-1} min^{-1} in the Rayonet-300 photoreactor.[53] The quantum yield for disappearance of **1** was 0.1. ^1H NMR spectra, ^{13}C NMR spectra of ^{13}CN-labeled **1** (δ 125.3), and ^{15}N NMR spectra of CN^{15}-labeled **1** (δ −132.2) revealed the formation of a mixture of many similar primary products, which were attributed to diastereoisomers of norcaradienes **4** and **6**.

(c) Other. CVCN, $1.0 \times 10^{-6} − 0.01$ M, was irradiated in degassed hexanes, benzene, toluene, and diethyl ether for times from 1 min to 10 h. The kinetics of changes in

(53) Moore, W. M.; Hammond, G. S.; Foss, R. P. *J. Am. Chem. Soc.* **1961**, *83*, 2789.
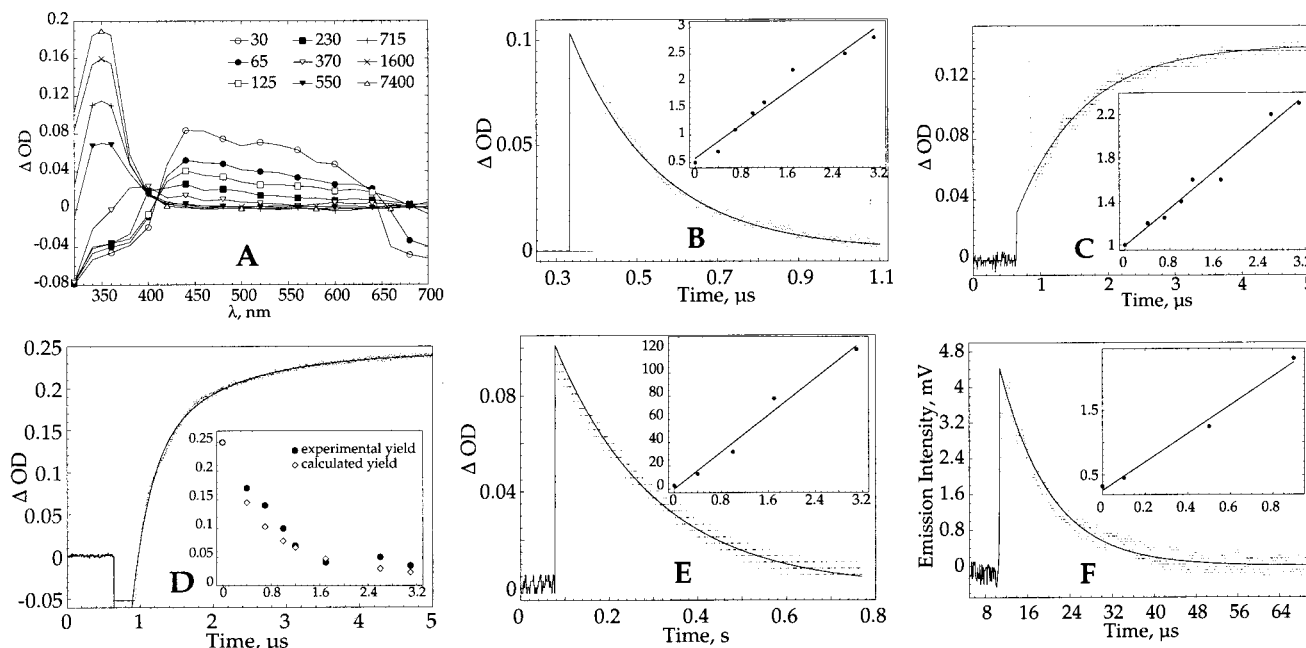
Figure 2. (A) Typical transient absorption spectra obtained on 266-nm excitation of 0.5 mM **1** in degassed diethyl ether at different times, ns; (B) Decay of absorption signal at 440 nm fitted monoexponentially; insert: $k^{440} \times 10^{-7}$, s^{-1} vs [O$_2$], mM; (C) Monoexponential rise of absorption signal at 350 nm (rise of **3** = total decay of **2**) with fitting curve (baseline was obtained with monitoring light off and subtracted); insert: $k^{350-rise} \times 10^{-6}$, s^{-1} vs [O$_2$], mM; (D) Rise of absorption signal at 350 nm fitted biexponentially (fast component 3×10^6 s^{-1} is the decay of the instrument response to fluorescence, slow component 0.8×10^6 s^{-1} is the rise of absorption of 350-nm species); insert: experimental and calculated yields of the 350-nm absorbing species **3** as a function of [O$_2$], mM; (E) Monoexponential decay of the 350-nm absorbing transient **3** with fitting curve; insert: $k^{350-decay}$, s^{-1} vs [O$_2$], mM; (F) Emission signal from singlet oxygen at 1270 nm fitted monoexponentially; baseline taken for the same solution purged with argon is subtracted; insert: $k^{1270} \times 10^{-5}$, s^{-1} vs [**1**], mM.

composition of the photolyzate was traced using UV–vis, NMR, TLC, and GC/MS. The same products in comparable yields were found in all cases.[54] Before PIOR, 3 major peaks of diarylacetonitrile **7**, 4 peaks of M$^+$ = 341 (unidentified), 2 peaks of stilbene **15**, and 1 peak of benzidine **12** (Table 5) were found in the GC/MS profile. This implies norcaradienes **4** and **6** produce **7**, **15**, and **12** at high temperature under helium. Oxygen-containing products **8**–**10** (Scheme 2) and **13** (Table 5) were detected only after the oxidation reaction had started, and their amounts grew steadily at the expense of the quantities of **7**, **15**, and **12**.

Laser Flash Photolysis. (a) T$_1$. Photolyses were carried out with the 8 ns pulse of a Nd:YAG laser exciting at 355 nm in benzene and toluene and 266 nm in hexanes, diethyl ether, and 1,2-dimethoxyethane. The results obtained using both λ_{exc} were identical. Typical transient spectra are shown in Figure 2A, and the rate constants are listed in Table 3. Negative absorption in the 300–400 nm and 650–700 nm (second harmonics) region is triggered by fluorescence (see later). We will focus on 266-nm LFP in diethyl ether. The 400–660 nm absorption band (λ_{max} = 440 nm) decayed with the lifetime of 180 ns under argon. Decay of this band was accelerated by oxygen, and the rate constant for quenching (k_{O_2}) was 7.7×10^9 M^{-1} s^{-1} (Figure 2B). Triplet excited states of aromatic amines often display broad and structureless absorption bands with maxima in the 400–500 nm region.[50,51] For example ^{3}DMA* absorbs at 460 nm and is quenched by oxygen in nonpolar solvents with the

rate constant of 1–2 × 10^{10} M^{-1} s^{-1}.[50,55] We attribute the 400–660 nm band to ^{3}**1***. We discarded CV$^\bullet$ and CV$^{\bullet+}$ because they both display a well-shaped absorption peak around 400 nm ($\epsilon \sim 2 \times 10^4$ M^{-1} cm^{-1}).[56] Another alternative, intermediate biradical-zwitterion **2** (Scheme 2), is unlikely because the yield of the 440-nm transient at $t = 0$ decreased only slightly with increasing oxygen concentration. Moreover, **2** is expected to absorb below 400 nm (see later).

(b) Quenching of T$_1$ by Oxygen. The value of $k_{O_2} = 7.7 \times 10^9$ M^{-1} s^{-1} is lower than the diffusion-controlled rate constant (k_{diff}) of 3×10^{10} M^{-1} s^{-1}, which is to be expected.[50,51,58] Emission of singlet oxygen was observed at 1270 nm (Figure 2F). The intensity of the signal extrapolated to $t = 0$ was used to estimate the average relative quantum yield of singlet oxygen ($\phi_{1\Delta g}$) as 0.3 in both aerated and oxygenated solutions. This falls into the typical 0.15–0.45 range for aromatic amines (e.g. $\phi_{1\Delta g}^{DMA}$ = 0.29 in aerated benzene).[50] Singlet excited states of aromatic amines are usually quenched by oxygen with k_{diff} regenerating the starting materials entirely.[50,58] Hence, the quantum yield for S$_1$ quenching by oxygen would be 0.18, which lowers ϕ_T to 0.65. Knowing $\phi_{1\Delta g}$ we can calculate the rate constant of energy transfer from ^{3}**1*** to oxygen $k_{1\Delta g}$ as 4.4×10^9 M^{-1} s^{-1}.[54] This value is consistent with 5.4×10^9 M^{-1} s^{-1} determined for DMA

(54) Jarikov, V. V. Ph.D. Dissertation, Bowling Green State University, Bowling Green, OH, 1999: also see Supporting Information.

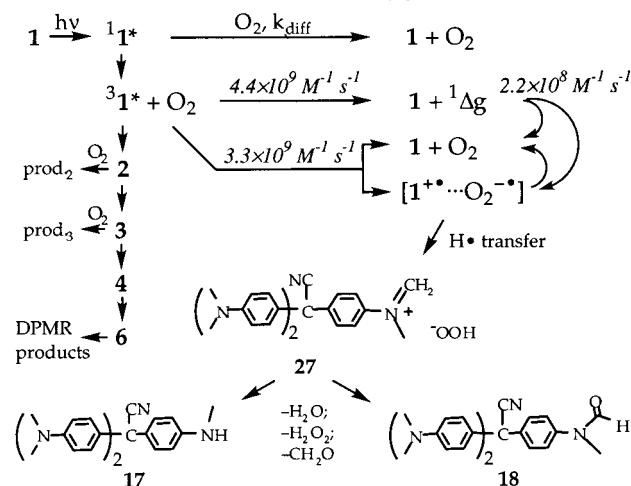(55) Wilkinson, F.; Brummer, J. G. *J. Phys. Chem. Ref. Data* **1981**, *10*, 809.
(56) Bhasikuttan, A. C.; Shastri, L. V.; Sapre, A. V.; Rama Rao, K. V. S.; Mittal, J. P. *J. Photochem. Photobiol. A: Chem.* **1994**, *84*, 237.
(57) Gijzeman, O. L. J.; Kaufman, F.; Porter, G. *J. Chem. Soc., Faraday Trans. 2* **1973**, *69*, 708.
(58) Wilkinson, F.; Abdel-Shafi, A. A. *J. Phys. Chem. A* **1999**, *103*, 5425.

Scheme 3. Irradiation of 1 in Rayonet-300 in the Presence of Oxygen

had a maximum at 350 nm and grew with a distinctly different 770-ns lifetime (Figs. 2C and 2D), which implies an intermediate is involved on the reaction pathway between T_1 and the 350-nm transient. An appealing interpretation of this is that the missing transient is biradical-zwitterion **2** (lifetime 770 ns), and the 350-nm species is biradical-zwitterion **3** (Scheme 2). Indeed, the rise and decay of a transient on the time scale expected for **2** was detected in the 350−420 region (Figure 2A, e.g., 370-ns point). However, measurements on the time scale up to several hundred nanoseconds were complicated by the appearance of a large negative signal of fluorescence peaking at 348 nm. This oversaturated the detector and caused the response to recover slowly with the rate constant of 3×10^6 s^{-1} (Figure 2D). This obscured the rise and decay of the absorption signal of **2** and the early part of the rise of **3**.[93] That both **2** and **3** absorb in the 320−420 nm region may be expected because a cyclohexadienyl radical formed by hydrogen atom addition to DMA displays a well-shaped peak at 370 nm,[67] and the absorption of substituted benzyl radicals is generally found in the 300−400 nm range.[68,69] Moreover, substituted cyclohexadienyl cations typically absorb in the 330−370 nm range,[70] and substituted benzyl and cyclohexadienyl anions absorb strongly in the 350-nm region.[71]

On the basis of the lifetimes of T_1 and **2**, quantum yields for T_1 ($\phi_T = 0.8$) and di-π-methane reaction (DPMR, $\phi_b = \phi_3 = \phi_4 = \phi_6 = \phi_{DPMR} = 0.1 = \phi$ for disappearance of **1** by NMR), and estimate of the rate constant k_c, it

in benzene,[50] and slightly higher, as expected,[50,58] than the maximum spin statistical rate constant of pure energy transfer based on the standard Porter model[57] (1/9)$k_{diff} = 3.3 \times 10^9$ M^{-1} s^{-1}. The difference between k_{O_2} and $k_{1\Delta g}$, k_{CT} describes isc and is 3.3×10^9 M^{-1} s^{-1}, which is lower than expected (1/3)$k_{diff} = 10 \times 10^9$ M^{-1} s^{-1} (e.g. $k_{CT}^{DMA} = 10.6 \times 10^9$ M^{-1} s^{-1} in benzene).[50] It is feasible that singlet oxygen is produced as a result of energy transfer from ^{3}**1***, which may also undergo physical quenching possibly via induced isc of the initial CT exciplex [^{3}**1***$^{\delta+}$···O$_2^{\delta-}$] to the ground-state complex that is unstable and unreactive. On the other hand, the CT exciplex may undergo net hydride transfer via H• transfer in the radical ion pair [**1**$^{•+}$···O$_2^{•-}$] to form ion pair **27** (Scheme 3).

(c) Quenching of O$_2$-$^1\Delta_g$. Aromatic amines efficiently quench singlet oxygen via CT exciplexes,[59,60] and this leads to both physical quenching and chemical reaction.[61−64] Amines react only if labile hydrogen atoms are α to the nitrogen atom.[62,65] The overall rate constant for quenching of singlet oxygen by **1** was evaluated from the dependence of the emission decay at 1270 nm on [**1**] and had a value of 2.2×10^8 M^{-1} s^{-1} (Figure 2F). This is close to the reported values for DMA, 1.3×10^8 M^{-1} s^{-1}, and DMT, 1.8×10^8 M^{-1} s^{-1} in methanol,[66] as well as for MG leucobase (MGH) in toluene, 2×10^8 M^{-1} s^{-1}.[65] The rate constant for the chemical reaction of MGH with singlet oxygen was 1×10^5 M^{-1} s^{-1}. This is consistent with the low quantum efficiency of < 0.01 for the oxidation of N-methyl groups, presumably via ion pair **27** (Scheme 3), determined in our product studies.

(d) ^{3}1* and Biradical-Zwitterions 2 and 3. The triplet excited state of **1** decayed with a 180-ns lifetime, giving rise to a species that had no absorption above 420 nm (Figure 2A and Table 3). The band at 320−400 nm

(59) Wilkinson, F.; Helman, W. P.; Ross, A. B. *J. Phys. Chem. Ref. Data* **1995**, *24*, 663.

(60) Gorman, A. A. *Adv. Photochem.* **1992**, *17*, 217.

(61) Martin, N. H.; Allen, N. W.; Cottle, C. A.; Marschke, C. K. *Photochem. Photobiol. A Chem.* **1997**, *103*, 33.

(62) Gollnick, K.; Lindner, J. H. E. *Tetrahedron Lett.* **1973**, 1903.

(63) Foote, C. S. In *Singlet Oxygen*; Wasserman, H. H., Murray, R. W., Eds.; Academic Press: New York, 1979.

(64) Young, R. H.; Brewer, D. R. In *Singlet Oxygen*; Ranby, B., Rabek, J. F., Eds.; Wiley: 1978; p 36.

(65) Stevens, B.; Kaplan, S. J. *Mol. Photochem.* **1979**, *9*, 205.

(66) Bellus, D. In *Singlet Oxygen*; Ranby, B., Rabek, J. F., Eds.; Wiley: 1978; p 61.

(67) Zador, E.; Warman, J. M.; Hummel, A. *J. Chem. Soc., Faraday Trans. 1* **1976**, *72*, 1368.

(68) Smirnov, V. A.; Plotnikov, V. G. *Russ. Chem. Rev.* **1986**, *55*, 929.

(69) Johnston, L. J. *Chem. Rev.* **1993**, *93*, 251.

(70) McClelland, R. A. *Spec. Publ.-R. Soc. Chem.* **1995**, *148*, 301.

(71) Cozens, F. L.; Ortiz, W.; Schepp, N. P. *J. Am. Chem. Soc.* **1998**, *120*, 13543.

(72) Malar, E. J. P.; Jug, K. *J. Phys. Chem.* **1984**, *88*, 3508, and references therein.

(73) Nonhebel, D. C.; Walton, J. C. *Free-radical Chemistry;* University Press: Cambridge, 1974.

(74) Ichinose, N.; Mizuno, K.; Otsuji, Y.; Caldwell, R. A.; Helms, A. M. *J. Org. Chem.* **1998**, *63*, 3176.

(75) Johnston, L. J.; Scaiano, J. C. *Chem. Rev.* **1989**, *89*, 521.

(76) Caldwell, R. A. In *Kinetics and Spectroscopy of Carbenes and Biradicals*; Platz, M. S., Ed.; Plenum Publishing Corp.: New York, 1990; p 77.

(77) Salem, L.; Rowland, C. *Angew. Chem., Int. Ed. Engl.* **1972**, *11*, 92.

(78) Neckers, D. C.; Linden, S.-M.; Williams, B. L.; Zakrzewski, A. *J. Org. Chem.* **1989**, *54*, 131.

(79) Glick, H. C.; Likhotvorik, I. R.; Jones, M., Jr. *Tetrahedron Lett.* **1995**, *36*, 5715.

(80) Klessinger, M.; Michl, J. *Excited States and Photochemistry of Organic Molecules;* VCH: New York, 1995.

(81) Scaiano, J. C.; Johnston, L. J. *Org. Photochem.* **1989**, *10*, 309.

(82) Bleasdale, C.; Jones, D. W. *J. Chem. Soc., Perkin Trans. 1* **1993**, *20*, 2441.

(83) Roth, W. R.; Klarner, F. G.; Siepert, G.; Lennartz, H. W. *Chem. Ber.-Recueil* **1992**, *125*, 217.

(84) Tang, T. H.; Lew, C. S. Q.; Cui, Y. P.; Capon, B.; Csizmadia, I. G. *J. Mol. Struct.* (*THEOCHEM*) **1994**, *111*, 149.

(85) Ford, W. E.; Rodgers, M. A. J. *J. Phys. Chem.* **1994**, *98*, 3822.

(86) Wilkinson, F.; Helman, W. P.; Ross, A. B. *J. Phys. Chem. Ref. Data* **1993**, *22*, 113.

(87) Gorman, A. A.; Rodgers, M. A. J. In *Handbook of Organic Photochemistry*; Scaiano, J. C., Ed.; CRC Press: Boca Raton, 1989; Vol. II.

(88) Ginzburg, O. F. *Sb. Statei Obshch. Khim.* **1953**, *2*, 1100; CA **1955**, 4596.

(89) Kubo, I.; Matsumoto, T. *Tetrahedron Lett.* **1984**, *25*, 4601.

(90) Yokoyama, M.; Ohteki, H.; Kurauchi, M.; Hoshi, K.; Yanagisawa, E.; Suzuki, A.; Imamoto, T. *J. Chem. Soc., Perkin Trans. 1* **1984**, *11*, 2635.

(91) Bardamova, M. I.; Usov, O. M. *Bull. Acad. Sci. USSR Div. Chem. Sci.* **1990**, *39*, 978.

(92) Shimamori, H.; Sato, A. *J. Phys. Chem.* **1994**, *98*, 13481.

Table 3. (1) Rate Constants Determined from LFP of 1 in Different Solvents; (2) 1 in Et$_2$O at Room Temperature: Lifetimes of the Assigned Intermediates and Their Rate Constants for Reaction with Oxygen

solvent	C$_6$H$_{14}$	PhH	MePh	Et$_2$O	DME[b]	species	S$_1$	T$_1$	**2**	**3**
440 nm decay,[a] s^{-1}	7.7×10^6	6.8×10^6	6.3×10^6	5.5×10^6	6.0×10^6	absorption, λ_{max}, nm	450–750, 610[g]	400–660, 440[f]	320–420, 390[f]	320–400, 350
350 nm rise,[a] s^{-1}	1.2×10^6	2.3×10^6	2.0×10^6	1.3×10^6	1.5×10^6	lifetime, ns	2.5[d]	180	770	3×10^8
350 nm decay,[a] s^{-1}	-	4.0	-	3.0	5.0	k_{O_2},[c] M^{-1} s^{-1}	3×10^{10}[e]	7.7×10^9	4.3×10^8	4×10^4

[a] Degassed solvent, single-exponential rate constants. [b] 1,2-Dimethoxyethane. [c] Rate constant for reaction with oxygen. [d] For MGCN in benzene, ref 26. [e] Diffusion-controlled rate constant, ref 51. [f] Obstructed by fluorescence signal peaking at 348 nm; unobstructed: T$_1$ = 350–740/405, **2** = two bands = 330–350 and 380–410 nm in benzene, ref 93. [g] For malachite green leucobase, leucohydroxide, and leuco methyl ether in cyclohexane, ref 32.

becomes possible to calculate the rate constants k_a, k_b, and k_d (Scheme 2; see Supporting Information). Rate constant k_a corresponds to the first step of DPMR, and k_c is the rate constant of the isc T$_1$ → S$_0$. Decay of T$_1$ under argon is accounted for by these rate constants. Similarly, k_b is the rate constant of the second step of DPMR, and k_d is the rate constant for the reversal of biradical-zwitterion **2** to **1**. The sum of these rate constants is given by the lifetime of **2**. On the other hand, we can estimate k_c based on the triplet lifetime of model compounds—aromatic amines, such as DMA, DMT, *N,N,N,N*-tetramethylbenzidine, *N,N,N,N*-tetramethyl-*p*-phenylenediamine, and the like—which is a rather constant value of 0.4–0.7 μs in nonpolar solvents.[50,51,92] Therefore, we take an average value of 2×10^6 s^{-1} for k_c. Thus $k_a = 3.5 \times 10^6$, $k_b = 2.6 \times 10^5$, and $k_d = 1 \times 10^6$ s^{-1}, and the absolute quantum yields for the processes a–d, are $\phi_a = \phi_2 = 0.5$, $\phi_b = \phi_3 = 0.1$, $\phi_c = 0.3$, $\phi_d = 0.4$.

The 350-nm transient **3** slowly decayed with the rate constant of 3 s^{-1} into a species that did not absorb light above 320 nm, presumably norcaradiene **4** (Figure 2E). The growth of 350-nm absorption (total decay of **2**) and the decay of it were accelerated proportionally to [O$_2$] in solution. The rate constant for reaction of **2** with oxygen was 4.3×10^8 M^{-1} s^{-1} (Figure 2C), and **3** was quenched with the rate constant of 4×10^4 M^{-1} s^{-1} (Figure 2E). The experimental yield of **3**, taken as ΔOD_{350} at its maximum value, decreased as oxygen concentration increased. Knowing k_a and k_b and rate constants for quenching of S$_1$, T$_1$, and **2** by oxygen, theoretical yields of **3** were calculated as a function of [O$_2$], which agree

(93) Confirmation of the LFP results and additional information was provided by pulse radiolysis studies of **1**, carried out by Drs. A. A. Gorman and I. Hamblett at Paterson Institute for Cancer Research, Manchester, UK.[54] The experimental setup has been described (Gorman et al. *Photochem. Photobiol.* **1994**, *59*, 389). Degassed benzene solutions of **1** (2.8, 1.4, and 0.28 mM) were irradiated with 50-ns electron pulses to produce ^{3}PhH* ($\tau_T = 3$ ns), which underwent triplet energy transfer with **1**. The unobstructed absorption spectrum of ^{3}**1*** was observed (350–740; $\lambda_{max} = 405$ nm) because the intensity of the fluorescence signal was nearly negligible. The triplet excited state of **1** decayed with the rate constant of 5×10^6 s^{-1}, and this was higher in the presence of oxygen. Concomitant with the triplet decay, two new absorption bands in the 330–350 and 380–410 nm regions were growing with the same rate as the rate of triplet decay. We assign these to biradical-zwitterion **2**. Later **2** disappeared and another new absorption (320–430; λ_{max}~360 nm) appeared with the rate constant of 1.3×10^6 s^{-1}. This we assign to biradical-zwitterion **3**. The absorption of **3** remained unchanged for over 50 μs. No measurement beyond this time was conducted. During both the LFP and pulse radiolysis experiments, an absorption formed within the pulse in the 450–700 nm region and decayed rapidly ($\tau \sim$ a few ns) within the late edge of the pulse. This absorption was of considerable intensity and may be due to formation and rapid recombination of the CV• •CN pair, although the mechanism for the formation of this radical pair differs for the two methods. However, it may also be due to absorption by ^{1}**1***. The exact absorption spectrum of this transient was impossible to measure due to time resolution of the instruments and low yield of the species.

well with the experiment (Figure 2D). Also, we can estimate ϕ_{DPMR} in the presence of oxygen. The product of ϕ_T, ϕ_a, ϕ_b, and ϕ_e provides an estimate of 2×10^{-4} in the aerated diethyl ether case and 4×10^{-5} for oxygenated benzene (see Supporting Information).[54]

(e) Summary.[93] On the basis of product studies described next, it appears reasonable to account for observations in LFP as following the di-π-methane reaction (Scheme 2 and Table 3). *Ipso*-coupling of two DMA rings in ^{3}**1*** produces triplet biradical ^{3}**2** with the rate constant of 3.5×10^6 s^{-1}. A value this low can be expected because, in the tetraaryldiene series, substitution of the phenyl rings by *p*-MeOPh and *p*-Me$_2$NPh slows the bridging (*ipso*-coupling) by factors of 40 and 2,600, respectively.[48] *Ipso*-coupling may be viewed as an intramolecular nucleophilic radical addition reaction in the *para*-position of an excited DMA chromophore by another DMA unit in **1**. Significant evidence exists that the lowest excited $\pi\pi$* states of aniline possess a pronounced quinoidal structure, and that this is reactive with respect to an addition reaction in the *para*-position, since the stabilizing effect of aromaticity is almost absent.[72] On the other hand, *ipso*-coupling resembles the photoinduced version of the Pschorr reaction.[73]

On the basis of E_T, average C–C bond dissociation energy in cyclopropane, and resonance energies of benzene ring and cyclohexadienyl radical, the bridging should be thermodynamically feasible and ^{3}**2** is likely generated in the ground triplet state. The 770-ns lifetime of **2** is a reasonable lifetime for a resonance stabilized triplet cyclopropyldicarbinyl ^{3}**2**, because the lifetimes of similar triplet 1,4-biradicals reported in the literature range from 0.01 to 100 μs, but are typically on the order of 0.1–1 μs.[74–76] These are usually determined by the rate of isc, which is controlled by spin–orbit coupling (SOC). The latter may be expected to be relatively small in ^{3}**2** according to the Salem–Rowland rules:[77] the average distance between the termini is substantially extended by the conjugation; rigid tricyclic spiro-structure of ^{3}**2** holds the atomic p orbitals in one plane and close to 60° with respect to each other; the singlet wave function may have a significant ionic contribution. The first two factors suppress and the third one promotes SOC. Therefore, we cannot predict whether triplet 1,4-biradical ^{3}**2** would undergo primarily isc and produce singlet biradical-zwitterion [^{1}**2** ↔ ^{Z}**2**] or ^{3}**2** would rather give rise to a triplet 1,3-biradical ^{3}**3**, which is substantially better stabilized by a captodative effect created by *p-N,N*-dimethylanilino- and cyano-substituents. Singlet biradical-zwitterion [^{1}**2** ↔ ^{Z}**2**] may cleave either an old C-DMA bond to generate a far more stable singlet biradical-zwitterion [^{1}**3** ↔ ^{Z}**3**] or new DMA–DMA bond to reform

Table 4. Mass Balance and Conditions of the Preparative Scale Irradiation experiments[a]

number	1	2	3[b]	4	5	6	7	8	9[b]	10[b,e]	11[b,c]
starting material	CVCN	CVCN	CVCN	CVCN	CVCN	CVCN	CVMe	CVBn	MGCN	TrCN	BFCN
[starting material], mM	5.6	7.0	7.2	6.4	8.4	6.9	8.1	6.3	8.4	6.8	0.3
additive[d]	-	-	-	c-C_6H_{10}	EtSH	O_2	-	-	-	-	-
starting material, g	3.29	2.78	2.75	2.53	3.36	2.74	3.05	2.92	3.0	1.84	0.1
total yield, g[g]	3.15	2.63	2.8	2.38	3.35	2.77	2.94	2.90	3.05	1.90	0.11
conversion, %	91	66	55	98	70	17	58	65	58	39	20
irradiation time, h	9	3	2.5	9.5	9	11	47	2.5	5	10	2
Σ yields of products, g	1.45	1.03	1.35	1.85	2.15	0.35	0.79	1.10	1.50	0.65	0.018
inseparable mix, g[f]	1.40	0.65	0.20	0.48	0.20	0.15	0.90	0.70	0.30	0.10	0.008

[a] Benzene solutions were irradiated in Rayonet-300 under argon, except for columns 6 and 10. [b] Heated under argon after irradiation. [c] Conditions are different due to limited solubility. [d] Molar ratios: **1**/cyclohexene(c−C_6H_{10}) = 1/1000; **1**/ethanethiol = 1/150; **1**/O_2 = 1/1.5. [e] Hexanes, Rayonet-254. [f] A large number of inseparable low-yield products represented mostly as a tail on the bottom portion of a TLC plate; also note that some of the most polar products are irreversibly bound to the silica gel of the column. [g] Recovered starting material + sum of the yields of products + inseparable mix.

Table 5. Yields of Products from Irradiation of 1 in Rayonet-300, Molar %[j]

no.	product\solvent	column number 1[a]	2[b]	3[c]	4[d]	5[e]	6[f]	7[g]	8[g,h]	9[g]	10[g]	11[g,i]
		PhH	PhH	PhH	PhH	PhH	PhH	Et_2O	Et_2O	C_6H_{14}	THF	MeCN
	conversion, %	91	66	55	98	70	17	90	80	25	50	95
9	Scheme 2	24	28	14	37	-	2	41	35	4	25	55
12	p,p'-Me_2NPh-PhNMe$_2$	7	3	8	7	63	-	5	5	5	2	7
7	Scheme 2	8	4	67	4	4	tr	3	4	35	3	2
8	Scheme 2	7	10	2	3	-	-	12	8	-	4	5
10	Scheme 2	17	21	6	tr	tr	10	16	27	3	1	5
13	p-Me_2NPhOH	9	7	2	21	-	12	3	10	2	1	4
14	Experimental Section	-	-	-	11	-	-	-	-	-	-	-
15	(p-Me_2NPh(CN)C=)$_2$	-	-	-	-	32	-	-	-	-	-	-
1′	MGCN	-	-	-	-	19	-	-	-	-	-	-
17	Scheme 3	2	tr	tr	tr	2	22	1	1	7	30	tr
18	Scheme 3	-	-	-	-	-	27	-	-	-	-	-
19	Michler's ketone	-	-	-	-	-	6	-	-	-	2	9
20	didemethylated CVCN	-	-	-	-	-	5	-	-	-	5	-
21	p-Me_2NPhCOOH	tr	tr	tr	-	-	5	tr	tr	-	2	-

[a] 9-h irradiation. [b] 3-h irradiation. [c] 2.5-h irradiation followed by heating under argon. [d] Trapping experiment with cyclohexene, different workup. [e] Trapping experiment with ethanethiol. [f] Under oxygen. [g] Columns 7−11: TLC and GC/MS-based study. [h] 254-nm irradiation. [i] Special conditions were applied; see text. [j] Columns 1−6: products separated by column chromatography; see Table 4 for the parameters of irradiation; "-" not detected; "tr" trace amount; see Supporting Information for minor products.

1. Alternatively, [3]**3** may undergo isc and produce [[1]**3** ↔ [Z]**3**] (Scheme 2).

The slow decay of **3** may be controlled either by cyclization of [[1]**3** ↔ [Z]**3**] or by the isc of [3]**3**. The latter may be disregarded because SOC in [3]**3** is expected to be efficient because (1) SOC-favoring conformations, where the atomic p orbitals are orthogonal and overlapping, are readily achievable; (2) ionic contribution to the singlet wave function is supposed to be large due to great stability of zwitterionic resonance form [Z]**3**. Therefore, the slow decay of **3** is controlled by low reactivity of the singlet biradical-zwitterion [[1]**3** ↔ [Z]**3**]. The cyclization may be viewed as Michael addition of α-cyanobenzyl carbanion to β,γ-unsaturated imminium cation.

Product Studies. (a) Standard Case: Benzene/ Argon/300 nm/Air Workup. In two separate preparative photolyses, degassed solutions of **1** in benzene were irradiated with polychromatic Rayonet-300 light for 3 and 9 h, respectively (Table 4, columns 1 and 2). Oxygen-containing products were formed upon exposure of the freshly irradiated solutions to air during the postirradiation oxidation reaction (PIOR). The products and the remaining **1** were separated, purified, weighed, and identified. The products were found to be the same with slight variations in yield (Table 5, columns 1 and 2). We suggest the vast majority of them came from a single intermediate, viz. norcaradiene **6**, and this is supported by experiments at different λ_{exc} and using different workup conditions. The major products may be rationalized as due to reactions of peroxy-biradical **11** and

cyclic perether **30**, which are the likely primary products of the reaction between norcaradiene **6** and oxygen (Scheme 2).[78] Peroxy-biradical **11** may be formed by reaction of biradical **5** with oxygen. The peroxy-radical of **11** may abstract H• from the adjacent position *ortho* to the amino group. This leads to rearomatization and produces diaryl(cyano)methyl hydroperoxide, which forms diaryl(cyano)methanol **9*** and subsequently benzophenone **9** (structure confirmed by X-ray crystallography). On the other hand, peroxy-radical may abstract H• from the neighboring *N*-methyl group, subsequently lose water, and form benzoxazine **8**. If the bond between the former central carbon atom and central benzene ring in **11** breaks, benzidine **12** and, eventually, benzoyl cyanide **10** are generated. Finally, cyclic perether **30** may be produced either directly or by cyclization of **11** and decompose in multiple ways producing **8**−**10**. Note isolated products account for ∼60−70% of the converted **1**. About 30−40% of the photolyzate consisted of a large number of inseparable low-yield products that most probably were formed from **6** by other minor, random oxidative routes.

(b) Solvent Effect. The generality of the photoreaction in solvents of different polarity was confirmed when the same products were identified and quantified in hexanes, diethyl ether, THF, and acetonitrile (Table 5). In acetonitrile, **1** was irradiated under special conditions. Since CV[+]CN^{−} was the major product, the preparative irradiation from which one could obtain and isolate other products was performed in 5 min increments after which

**Table 6.   Yields of Products from 350-nm Irradiation of 1 and Electron Acceptors (e⁻A) in Degassed Benzene, Molar %[a]**

e⁻A, ratio	-	DCA, 1:1	DCB, 1:1.5	BP, 1:1	BP, 1:1.5[b]
c, %/t, h	50/20	29/20	25/20	20/2	100/20
9	-	-	-	5	-
12	16	10	2	4	4
7	71	65	61	5	28
8	-	-	-	21	3
25[c]	5[d]	9[d]	3[d]	80	100
22	15	7	3	3	5

[a] [**1**] = 3×10^{-3} M, TLC and GC/MS-based study; average of several experiments; ratio = **1**: e⁻A; c = conversion, recovered **1** contains some mono-demethylated compound; t = irradiation time; "-" = not detected. [b] All of the products are dimerized and trimerized; see text. [c] Yield of dimeric and trimeric products; see text. [d] **46**: CVCN dimer (Ar)MeN−CH₂−CH₂−NMe(Ar).

the ion pair was allowed 30 min to reform **1** via a thermal reversion reaction ($k = 7.5 \times 10^{-4}$ M⁻¹ s⁻¹). Variations in yields of the major products may have resulted due to the effect of the solvent on PIOR. The formation of large amounts of demethylated CVCN **17** in THF and the preferable formation of **7** over **9** in hexanes remain to be explained. The only drastically different distribution of products was observed when dichloromethane, chloroform, and carbon tetrachloride were used as solvent. The sole product formed in these solvents was CV⁺Cl⁻, and no fading of the dye was observed. Likely **1*** underwent oxidative quenching by the solvent producing **1**⁺, which led to CV⁺.[14,54]

(c) Effect of λ_exc. When irradiated at 254 nm, variations in the yields of products obtained in diethyl ether turned out to be insignificant (Table 5, columns 7 and 8). This may indicate internal conversion of S_2 to S_1 occurs first. However when irradiated with 350-nm light, the yield of **7** increased to over 70%, former major products **8−10**, and **13** were not detected, yield of benzidine **12** increased to 16%, and a new product, arylacetonitrile **22**, was found in a comparable 15% yield (Table 6). Since we hypothesize norcaradiene **6** absorbs strongly in the 340−400 nm region, the changes observed are likely due to photochemical reactions of **6**, which was present in photostationary concentration. Either **6** undergoes cleavage of one cyclopropane bond (83%) rearranging to **7** probably via H[1,2] shift in biradical **5**, or two bonds are cleaved (17%) forming a well-stabilized carbene **23** and **12**. Carbene **23** abstracts two hydrogen atoms, most possibly from *N*-methyl groups of **1** and forms **22** (Scheme 2). The formation of carbenes and isomerizations to toluenes are the two characteristic processes resulting from the photoinduced reactions of norcaradienes.[79] The photochemical reactions of **6** are manifested in the yields of products obtained in 300-nm photolysis. In that case, the longer the irradiation time, the larger the yields of biphotonic products **7** and **12**. This comes at the expense of the monophotonic products **8−10** (compare columns 1 and 2, Table 5). Note we have accounted for ~95% of the converted **1**.

(d) Effect of Workup. Instead of exposing a benzene solution of photolyzate to air, it was boiled under argon for several hours until the benzene distilled, and the viscous residue was subsequently heated to 105−120 °C. Product distribution implied that norcaradiene **6** produced **7** thermally (Table 5, column 3). Nevertheless, some **6** remained and was oxidized since products **8−10** were isolated from the photolyzate. In this case the

Scheme 4.   Trapping with Ethanethiol: Formation of 1′
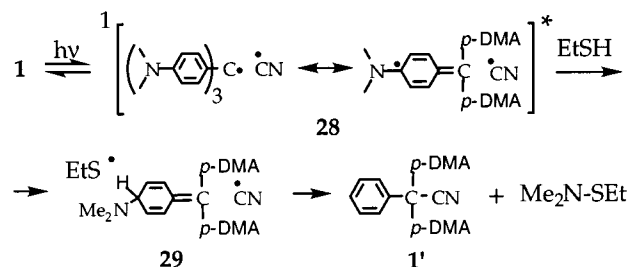
isolated products accounted for ~90% of the converted **1** (Table 4, column 3).

(e) Effect of Oxygen. Preparative photolysis in oxygenated benzene (Table 4, column 6) led to N-demethylation and oxidation of the *N*-methyl groups of **1** (Table 5, column 6) with low quantum efficiency (~0.01). The ion pair **27** was the likely primary product, which led to final products **17** and **18** via several pathways (Scheme 3). Based on the amount of isolated **9**, ϕ_{DPMR} in oxygenated benzene is ~2×10^{-4}, which is consistent with the predicted 4×10^{-5}. About one-third of the photolyzate consisted of a large number of polar compounds that could not be separated and that might have been produced both in reaction with H₂O₂ and excitation of the oxygen-containing products.[54]

(f) Trapping Experiments. Two experiments were carried out in an attempt to trap radical and carbene intermediates and isolate the corresponding products. Trace amounts of two trapped-carbene products were detected in the presence of cyclohexene (Table 4, column 4), while the DPMR persisted as indicated by the distribution and the yields of products (Table 5, column 4). Interestingly, after immediate removal of solvent, we obtained a yellow crystalline solid in ~70 wt % yield. Although the MS and NMR analysis support our assumption, we are unable to conclusively show that the solid was a mixture of the norcaradienes **4** and **6** because they were formed as diastereoisomeric mixtures and both started to react with oxygen promptly during and after isolation. The sizable 10% increase in the yield of benzophenone **9**, the formation of a new major product, pyrocatechol **14** (structure confirmed by X-ray crystallography), and replacement of benzoyl cyanide **10** by aminophenol **13** may be rationalized as being due to variations in the radical PIOR triggered by the different workup procedure. Pyrocatechol **14** might have come from the oxidation of norcaradiene **4**.

In another experiment (Table 4, column 5), the addition of a good hydrogen atom donor, ethanethiol, in 150-fold excess gave rise to an unexpected array of isolated products (Table 5, column 5), accounting for ~90% of the converted **1**. The photolyzate was exposed to air immediately after the irradiation was completed, but no oxygen was incorporated into the final products. Only a trace of the trapped-carbene product was detected, and 1% of CV leucobase (*p*-Me₂NPh)₃CH was isolated. The formation of MGCN may have resulted from the radical substitution reaction (Scheme 4), which leads to the conclusion that the C−CN bond homolysis takes place with $\phi \geq 0.02$. Since the intervention of the homolytic bond cleavage has not been seen elsewhere in our study, we assume it is a singlet state reaction and the recombination of the singlet radical pair within the solvent cage

is rapid. The 10-fold increase in the yield of benzidine **12** and isolation of a new product stilbene **15** in 1:2 molar ratio to **12** are difficult to rationalize. Two former central carbon atoms make up a double bond in **15**, implying **15** and **12** originate from a dimeric intermediate. This requires further investigation.

(g) Effect of Electron Acceptors. Degassed benzene solutions of **1** were irradiated under identical conditions ($\lambda_{exc} = 350$ nm) in the presence of 9,10-dicyanoanthracene (DCA), 1,4-dicyanobenzene (DCB), and benzophenone (BP). Absorption measurements provided no evidence for complex formation between the acceptors and **1** in the ground state up to decimolar concentration. Results of the control experiment have been discussed. The quantity of DPMR products decreased with increasing oxidative power of the electron acceptor suggesting the DPMR is in competition with the e⁻T reactions (Table 6). **(i) DCA and DCB.** About 90% of the incident light was absorbed by DCA in one case and by both **1** and DCB in approximately equal amounts in the other. Product yields displayed rather minor deviation from those in the control experiment. Formation of **7**, **12**, and **22** was suppressed since both **1** and norcaradiene **6** had to compete for light with DCA or DCB. Also, **1*** may reduce DCA and DCB, and DCA* and DCB* can be reduced by **1** forming the radical ion pair. We suggest **1**·⁺ underwent an efficient in-cage back e⁻T with both cyanoaromatic radical anions to reform the starting materials. However, in the case of DCA, one-fourth of the starting material was converted into 9-cyanoanthracene. The latter was likely produced upon typical proton transfer from **1**·⁺ to DCA·⁻, followed by e⁻T and subsequently by cleavage of cyanide anion. The formation of an initial exciplex might have taken place because it is typical for aromatic hydrocarbons and dialkylanilines.[80] **(ii) Benzophenone.** At the outset ∼90% of the incident light was absorbed by BP, but later norcaradiene **6** competed for the 350-nm light producing **7**, **12**, and **22**. Among the DPMR products, the products of the photochemical reactions of **6** prevailed in the 20-h photolysis, while the products of the oxidation of **6** predominated in the 2-h run (Table 6). Various dimers and trimers **25** were found in the photolyzate. The photoreduction of BP by DMA has been shown to involve the triplet exciplex followed by formation of the radical ion pair, which undergoes facile proton transfer.[80] Therefore, we assume efficient proton transfer to the BP·⁻ from the *N*-methyl group of **1**·⁺ and from radical cations of photoproducts occurred. The *N*-methyl radicals of **1** and DPMR products dimerized, cross-coupled, and coupled with a benzhydryl radical. About one-third of the BP was converted into benzhydrol, likely by the disproportionation reaction of two benzhydryl radicals.[56]

II. Other TAM Leuco Dyes. (a) Crystal Violet Leucomethyl (1a, Scheme 2). We postulated the photochemical behavior of **1a** would elucidate the mechanistic roles of the zwitterionic structures as well as the homolysis of the C−X bond, and that norcaradiene **6a** might turn out stable to oxidation. The quantum yield for disappearance of **1a** in C₆D₆ was 0.005. Steady-state photolyses indicated inefficient formation of multiple products and occurrence of a PIOR. In the preparative experiment, **1a** was irradiated under 300-nm light for 47 h (Table 4), and a large number of inseparable compounds formed in low yields and constituted about 55% of the photolyzate. The other 45% were separated and

Table 7. Yields of Major Products from 300-nm Irradiation of 1a and 1b in Degassed Benzene, Molar %[b]

	CVMe			CVBn	
no.	structure	yield	no.	structure	yield
12	p,p'-(Me₂NPh-)₂	1	**12**	p,p'-(Me₂NPh-)₂	5
7a	Scheme 2	10	**10b**	Scheme 2	27
17a	N-demethylated CVMe	11	**24**	p-Me₂NPhCH=CHPh	5[a]
9a*	Scheme 2	3	**9b**	olefin[c]	12[a]
8a	Scheme 2	10	**8b**	Scheme 2	16
13	p-Me₂NPhOH	8	**13**	p-Me₂NPhOH	13
26a*	Scheme 2	9	**26b**	olefin[c]	10[a]

[a] *E*/*Z* isomers. [b] See Table 4 for the conditions of irradiation. [c] **9b** and **26b** are olefins obtained by spontaneous dehydration of **9b*** and **26b*** respectively (Scheme 2).

products identified (Table 7), which included diarylethanol **9a***, diarylethane **7a**, benzoxazine **8a**, and a new product, deaminated diarylethanol **26a*** (Scheme 2). Compound **26a*** probably resulted from an alternative cyclization route of peroxy-biradical **11a**, producing cyclic perether **16a**, which subsequently underwent rearomatization by deamination, likely the result of the Ph−O being a stronger bond than Ph−N.[51] The formation of a significant amount of *N*-demethylated CVMe **17a** is normal under the conditions of such a prolonged irradiation ($\phi \sim 6 \times 10^{-4}$).[28] On the basis of the amount of the products derived from norcaradiene **6a**, we estimate that about 50% of the **1a** converted underwent DPMR, 10% suffered N-demethylation, and 40% was decomposed, probably in multiphotonic and bimolecular events.

We suggest ³**1a*** gives rise to biradical ³**2a**, which appears to be of similar stability to ³**2**. Therefore ³**1a*** should undergo bridging as efficiently as ³**1***. Biradical-zwitterion **2a** may prefer to rearrange by breaking of a newly formed *ipso*-bond and reform the starting material. This results because the driving force for going from **2a** to **3a** is significantly smaller than going from **2** to **3** on the radical pathway, and especially smaller on the zwitterionic pathway (Scheme 2). The (1-methyl)-*p*-aminobenzyl terminus of biradical ³**3a** is substantially less stabilized than the (1-cyano)-*p*-aminobenzyl terminus of ³**3** due to shorter delocalization and the absence of captodative effects. Moreover, the (1-methyl)-*p*-aminobenzyl anion of zwitterion ᶻ**3a** is far less stable than the (1-cyano)-*p*-aminobenzyl anion site of ᶻ**3**.

(b) Crystal Violet Leucobenzyl (1b, Scheme 2). The photochemistry of CVBn was studied with the initial assumption that C−Bn bond homolysis (dissociation energy ∼200−250 kJ/mol) should easily occur.[51] However, upon 300-nm irradiation in degassed benzene (Table 4), no products deriving from C−Bn bond homolysis were detected. Moreover, the DPMR ($\phi = 0.12$ in C₆D₆) persisted as seen from the structures of isolated products (Table 7). Steady-state photolysis revealed a picture identical to the CVCN case. We suggest ³**1b*** suffers *ipso*-coupling of two DMA rings as efficiently as **1** and **1a** and produces biradical-zwitterion **2b**. In terms of the stabilizing effect of cyano, methyl, and benzyl substituents on radical and anionic centers, biradical-zwitterion **3b** is slightly more stable than biradical-zwitterion **2b**, similar to the situation with **3a** and **2a**. Therefore, benzyl derivative **2b** is expected to behave similarly to methyl derivative **2a**, i.e., mostly reform starting material while affording little **3b**. However, since **1b** is about as reactive as **1**, we assume a kinetic effect, such as the specific steric environment of the cyclopropane ring in **2b**, overpowers the thermodynamics of **2b** → **3b**. Norcaradiene **6b** was

Scheme 5. Irradiation of Malachite Green Leuconitrile (1′) in Benzene, 300 nm: Two Types of *Ipso*-Coupling; Products and Yields, Molar %
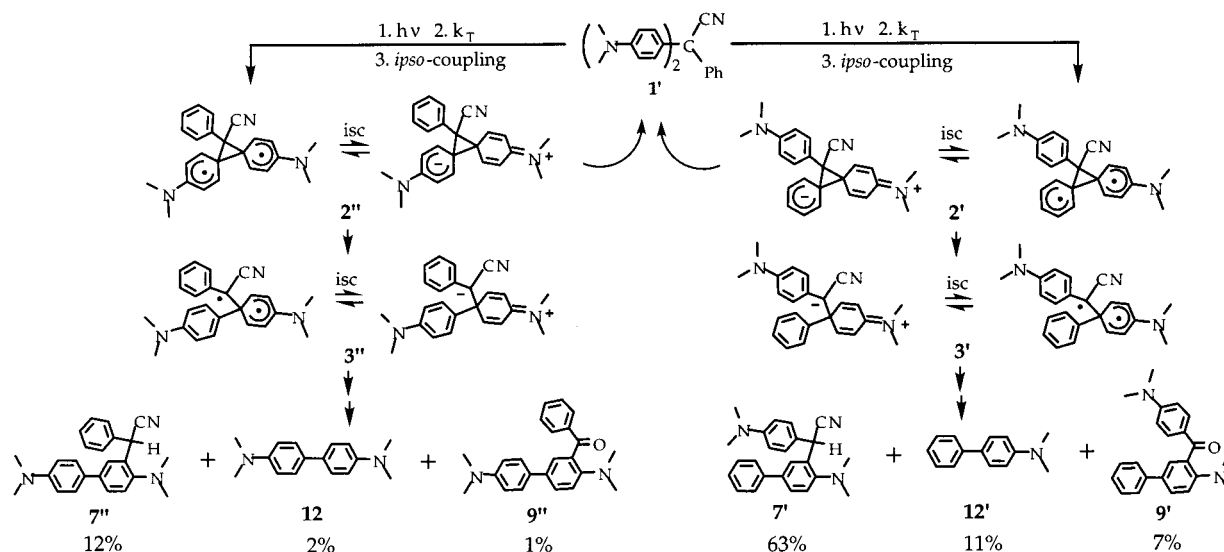
oxidized into diaryl(benzyl)carbinol **9b***, which dehydrated, giving rise to olefin **9b**. On the other hand, **6b** was transformed into benzoxazine **8b**, phenylacetophenone **10b**, and stilbene **24**. The deamination reaction proceeded in the same way as in the CVMe case and provided olefin **26b** after dehydration of deaminated diaryl(benzyl)carbinol **26b***. Separated products of DPMR accounted for ∼70% of the converted **1b**; therefore, like in the CVCN case, we assume ∼95% of the converted **1b** was consumed in the DPMR.

(c) Malachite Green Leuconitrile (1′, Scheme 5). Similar to **1**, **1′** gave rise to the yellow color when irradiated in degassed nonpolar solvents and polymer matrixes. In the preparative photolysis, **1′** was irradiated with 300-nm light in degassed benzene, and ϕ_{DPMR} was 0.06 (Table 4). After irradiation, benzene was distilled and photolyzate was heated under argon. The isolated products accounted for >90% of the **1′** that had been converted, and their yields and structures were analogous to those of the photoproducts of **1** (Table 5, column 3, Scheme 5). The presence of the unsubstituted phenyl ring in the structure of **1′** allowed differentiation of the efficiencies of two types of *ipso*-coupling processes: DMA–DMA and DMA–Ph. The biradicaloid structures of intermediate **2″** are stabilized by two dimethylamino groups compared to one in **2′** (Scheme 5). Stabilization is brought about by removal of ∼25% of the spin density from the carbon-centered radical by an α-amino substituent.[73] However, zwitterionic resonance structures of **2″** are less stable than those of **2′** because the dimethylamino group destabilizes the negative charge on the cyclohexadienyl ring. In intermediates of type **3**, the relative input of zwitterionic structures should be large, hence **3′** and **3″** may be isoenergetic. The yields of **9′**, **12′**, and **7′**, which originated from biradical-zwitterion **2′**, are five times larger than the yields of **9″**, **12**, and **7″**, which came from **2″**. Therefore, either biradical-zwitterion **2″** undergoes the reversal to the starting material more readily than **2′**, or **2″** → **3″** is inhibited compared to **2′** → **3′**.[54]

(d) Basic Fuchsin Leuconitrile (Scheme 6). After the saturated solution of BFCN in degassed benzene (λ_{max} = 296 nm) was irradiated in the Rayonet-300, the solvent was removed and the residue heated to 120 °C under

Scheme 6. Irradiation of BFCN in Benzene, 300 nm
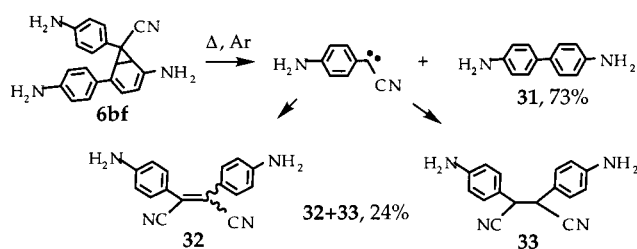
Scheme 7. Irradiation of 1t in Hexanes in Rayonet-254
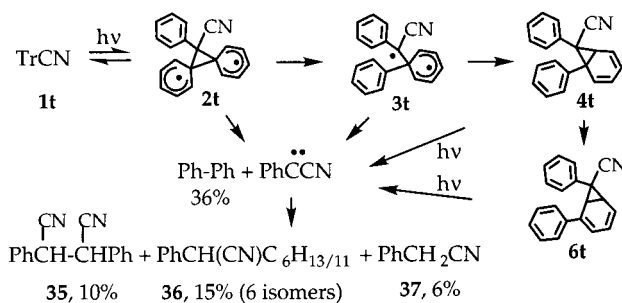
argon (Table 4). Three major products were separated (Scheme 6). Before heating, the yield of benzidine **31** was about 10-fold lower than was observed after heating, while stilbene **32** and ethane **33** were absent. Therefore, we suggest the formation of these products happened during the heating of the melted residue, most probably via a thermal formation of 4-anilino(cyano)carbene and **31** from norcaradiene **6bf**. Stilbene **32** resulted from direct coupling of two carbenes, and **33** was the product of hydrogen atom abstraction by carbene followed by the dimerization of the produced radical. Quite possibly, the carbene was consumed in other reactions that led to unidentified products and depleted the yield of **32** and **33**.

(e) Trityl Nitrile (1t, Scheme 7). Okamoto, Shi, and Takamuku studied the photochemistry of triphenylmethyl derivatives, including **1t**, in methanol.[42] According to them, ¹**1t*** underwent α,α-elimination of biphenyl and formed a singlet (cyano)phenylcarbene, which inserted

into the OH bond of methanol.[47] They accounted for 38% of the converted **1t** and provided no information on the other photoproducts. It was appealing to compare the photochemistry of the simplest in the series of TAM nitriles with the photochemical reactions of CV, MG, and BF leuconitriles in nonpolar solvents. Trityl nitrile was irradiated in degassed hexanes (λ_{exc} = 254 nm), and the photolyzate was heated under argon after irradiation (Table 4). Four of the products obtained pointed to the intermediacy of cyano(phenyl)carbene in ~40% yield (Scheme 7). Ethane **35** resulted from the H• abstraction by the carbene followed by dimerization of the radical produced. Were it to abstract a second hydrogen atom, it would produce phenylacetonitrile **37**. Insertion of the carbene into the C–H bonds of hexanes gave rise to six isomeric alkyl(phenyl)acetonitriles **36**. The origin of the carbene and biphenyl, whether they came from **2t/3t** or from the excitation of **4t/6t**, as well as the multiplicity of the reaction requires additional investigation (Scheme 7). We suggest both singlet and triplet carbenes are involved because products of both insertion into the C–H bond (15%) and H• abstraction (26%) were isolated. An interesting finding was isolation of seven isomers of **1t** in 30% yield. Column chromatography afforded three mixtures of 2–3 compounds each, which, unfortunately, could not be separated. All of the isomers had the molecular ion of **1t**. On the basis of TLC and MS, we suggest these isomers may be norcaradienes **4t** and **6t** and their valence tautomers.[54]

Conclusions

(a) Alternative Mechanisms. (i) Carbene. One possible alternative to the DPMR is the α,α-elimination of benzidine **12** from biradical-zwitterions **2** and **3** and formation of carbene **23**. However, on the basis of observations in the photolysis, structures of the products of **1** irradiated in nonpolar solvents at 300 nm, and most of all trapping experiments, the α,α-elimination was discarded. Note that the products, which we assume originated from the chemistry of free carbene **23**, were produced only when **1** was subjected to 350-nm (not 300-nm) irradiation and attributed to the photochemistry of **6** (λ_{max} ~ 370 nm). **(ii) Crystal Violet Radical.** Another plausible alternative to the DPMR involves initial C–CN bond homolysis (dissociation energy ~ 300–320 kJ/mol)[51] to produce CV•, which then undergoes a photochemical reaction. The homolysis is energetically favorable in both excited states. Many workers have studied the photochemistry of TAM radicals.[69,81] We discarded this mechanism since none of the isolated products are the expected products of the photochemical reactions of CV•. Nevertheless, isolation of MGCN in the trapping experiment with ethanethiol combined with the observation of a very short-lived species (low yield; lifetime ~ 1 ns; absorption 400–700 nm)[93] in nanosecond LFP leads us to suggest that one of the relaxation routes of ^{1}**1*** is indeed the C–CN bond homolysis which is either inefficient or followed by in-cage recombination. **(iii) Dark Reaction.** Norcaradiene, cycloheptatriene, norbornadiene, and toluene are valence tautomers[82] and can be converted into one another by hydrogen and carbon migrations and pericyclic reactions.[52,83] The appearance of the yellow band (340–400 nm) and dark reaction (its growth in the dark) might be due to transformation of norcaradienes **4** and **6** into conjugated diarylcycloheptatriene structures.

Norcaradienes with electron-withdrawing substituents at the 7 position are known to undergo this equilibrium reaction spontaneously.[84] However, since ring expansion products or products of the norbornadiene kind have not been found in the present study, we assume these reactions did not occur.

(b) Summary.[93,94] We suggest in solvents with $\epsilon \geq$ ~5 ionization of **1** occurs from S$_1$, while in solvents with $\epsilon <$ ~30–35 the DPMR originates from T$_1$ (Scheme 1). We propose homolysis of the C–CN bond occurs in all the solvents, and the singlet radical pair promptly reforms **1**. The DPMR is followed by C[1,5] migration producing the critical intermediate, norcaradiene **6**. The latter undergoes oxidation in air, rearranges to diarylaceto-nitrile **7** thermally, and produces **7** and carbene **23** under 350-nm light. The generality of DPMR is shown for different solvents, λ_{exc}, and TAM leuco dyes. The presence of oxygen quenches the DPMR and leads to the oxidation of *N*-methyl groups of **1**. About half of the quenching of ^{3}**1*** produces singlet oxygen, which is in turn quenched by **1**.

Experimental Section

Materials and Equipment. Reagents and solvents were purchased from Aldrich. Benzene was distilled from sodium/benzophenone and cyclohexene was distilled under vacuum. Solvents used without purification were either spectrophotometric or HPLC grade. Ethyl acetate and hexanes (Pharmco) were distilled from glass. Elemental analysis was carried out by Atlantic Microlab Inc. HRMS was performed at the University of Illinois Urbana/Champaign, School of Chemical Sciences. Column chromatography and preparative TLC were performed using Scientific Adsorbents silica gel (40 μm, 32–63 μm) and silica gel plates (250 and 2000 μm; 5 to 17 μm; 60 Å). Melting points were not corrected.

Irradiation of Samples. Photolyses were performed under a dry argon atmosphere. A Rayonet RPR-100 photoreactor (a merry-go-round apparatus) equipped with 14 bulbs was used. Three types of GE bulbs were employed: 300-nm filter-coated (21 W), 350-nm filter-coated F8T5 (24 W), and 254-nm G8T5 (8 W) low-pressure mercury UV bulbs. The emission distribution spectrum for the 300-nm bulbs had a Gaussian shape with a maximum at 300 nm. At 250 and 350 nm, the intensity was 0 and 3%, respectively. About 90% of the intensity was concentrated in the 280–320 nm region. The emission spectrum for the 350-nm bulbs was centered at 350 nm and had 0 and 4% of the intensity at 310 and 400 nm, respectively. These bulbs emitted 90% of their energy in 330–370 nm range. The 254-nm bulbs produced essentially monochromatic light that provided 90% of irradiation intensity around 254 nm. Quartz 1000 mL and 250 mL round-bottom flasks (Ace Glass), 10 mL quartz test tubes, NMR tubes, and long-neck quartz fluorescence cuvettes all dried and sealed with a rubber septum were used as photolysis vessels. Solutions in the flasks were degassed with dry argon gas for 2 h prior to, and continuously during, a preparative photolysis and stirred briskly with a magnetic stirrer. Dry oxygen was blown into the flask during irradiations carried out under oxygen.

Isolation and Quantification of Photoproducts. The disappearance of starting material and appearance of products was monitored by TLC and GC/MS. After irradiation, the solutions were either exposed to air or solvent was distilled under argon. In the latter case, the dry residue was heated to 110–120 °C for 5–10 h under argon. With exposure to air, oxidation occurred, completion of which took from several hours to a day. After the solvent was removed, the resulting solid was dissolved in the minimal amount of chloroform and subjected to flash column chromatography using hexanes:ethyl

(94) For a recent review, see Jarikov, V. V.; Neckers, D. C. *Adv. Photochem.* **2001**, *26*, in press.

acetate (from 20:1 to 1:1). The unreacted starting material and products were separated, purified, weighed, and identified by ^{1}H, ^{13}C, and 2-D NMR, mass, IR, and UV−vis spectroscopy, elemental analysis, HRMS, and TLC (X-ray crystallography for **1**, **9**, and **14**). In the cases of CVMe, BFCN, and TrCN, photolyzate was separated into crude products by chromatography. Because of the difficulty of purification, some or most of these were identified as is, on the basis of TLC, MS, and NMR. In the experiments with different solvents, different λ_{exc}, and electron acceptors, which were analyzed by GC/MS, decane was used as an internal standard. In a trapping experiment with cyclohexene most of the solvent was immediately removed in vacuo after irradiation to provide ca. 1.8 g of yellow crystalline solid (70 wt %) and 0.8 g of brown amorphous residue. The solid had a very limited solubility in dichloromethane, but in a few hours all of it turned into brown amorphous mass that could be dissolved in 5 mL of dichloromethane.

Fluorescence Measurements. Fluorescence spectra were recorded with a SPEX Fluorolog 2 in perpendicular geometry using 1 cm quartz cuvette, and were corrected (band-pass 2.8 nm). All ϕ_{fl}'s are relative to *N,N*-dimethylaniline in benzene as the external standard.[51] Solutions were saturated with either argon or air. Generally, ϕ_{fl}'s were found to be fairly independent of λ_{exc}, and averaged values are reported. The fluorescence excitation spectra of **1** are found to be identical with the ground-state absorption spectra.

Laser Flash Photolysis. The setup has been described.[85] Photolyses were performed with the third (355 nm, 55 mJ/ pulse at maximum) and the fourth harmonic (266 nm, 3−5 mJ/pulse) of a Continuum Surelite I Q-switched Nd:YAG laser which provided 8 ns pulses. Argon, argon−air mixtures of known composition, air, or oxygen were purged through the 2.5-mL sample solutions, which were contained in 1 × 1 cm fluorimetry cuvettes. To minimize the absorption by the photoproducts, the solutions were stirred after each shot and refreshed every 5 shots in 355-nm experiments, and every 25 shots in 266-nm experiments.

Singlet Oxygen Luminescence. Singlet oxygen was generated from solutions of **1** in diethyl ether using the laser instrument described above (λ_{exc} = 266 nm). Time-resolved luminescence (1270 nm) signals were measured using germanium photodiode-amplifier system cooled to 77 K. A complete description of instrumentation and methodology is given elsewhere.[95] A solution of benzophenone in diethyl ether, the quantum yield of singlet oxygen of which was taken as 0.4, was used as a standard.[86,87] The lifetime of singlet oxygen in pure diethyl ether was taken as 30 μs.[87] To eliminate the scattered laser light and emission artifacts, the decay profiles obtained under argon were subtracted as a baseline from the profiles obtained in aerated diethyl ether.

Synthesis. Tris(*p-N,N*-dimethylaminophenyl)acetonitrile (CVCN), bis(*p-N,N*-dimethylaminophenyl)phenylacetonitrile (MGCN), and tris(*p*-aminophenyl)acetonitrile (BFCN) were synthesized by treating crystal violet chloride, malachite green oxalate monohydride, and pararosaniline base, respectively, with potassium cyanide in water in the presence of HCl. Tris-1,1,1-(*p-N,N*-dimethylaminophenyl)ethane (CVMe) and tris-1,1,1-(*p-N,N*-dimethylaminophenyl)-2-phenylethane (CVBn) were made in THF via the corresponding methylation by methyllithium and benzylation by benzylmagnesium bromide of crystal violet tetraphenylborate. Triphenylacetonitrile was made by reaction of trityl cation, generated in-situ from triphenylmethanol in warm acetic anhydride and tetrafluoroboric acid, with KCN. All the compounds were purified by column chromatography followed by cold crystallization from methanol−dichloromethane and then from hexanes− dichloromethane. In some cases **1** was purified from its *N*-demethylated derivatives by treatment with lauryl chloride followed by recrystallization from the hexanes−chloroform.

Tris(4-*N,N*-dimethylaminophenyl)acetonitrile (1)[29] (94% yield): for X-ray crystallography structure report see ref 54;

^{1}H NMR (400 MHz, CDCl$_3$) δ 7.06 (d, J = 8.4 Hz, 6H), 6.64 (d, J = 8.4 Hz, 6H), 2.93 (s, 18H); ^{13}C NMR (APT, 50 MHz, CDCl$_3$) δ 149.6, 129.4, 129.1, 124.6(CN), 111.9, 55.0, 40.4; IR (KBr) cm^{-1} 2885, 2233(CN), 1608, 1518, 1354, 814; MS (EI, 70 eV) 398, 278(b), 262, 240. Anal. Calcd for C$_{26}$H$_{30}$N$_4$: C, 78.35; H, 7.58; N, 14.05. Found: C, 78.33; H, 7.57; N, 13.99; mp = 293− 294 °C.

Bis(4-*N,N*-dimethylaminophenyl)phenylacetonitrile (1′)[29] (96% yield): ^{1}H NMR (200 MHz, CDCl$_3$) δ 7.35−7.21 (m, 5H), 7.05 (d, J = 9.0 Hz, 4H), 6.64 (d, J = 8.8 Hz, 4H), 2.93 (s, 12H); ^{13}C NMR (APT, 50 MHz, CDCl$_3$) δ 149.7, 141.6, 129.4, 128.6, 128.3, 128.2, 127.5, 124.2(CN), 111.9, 55.8, 40.3; IR (KBr) cm^{-1} 2887, 2803, 2231(CN), 1609, 1519, 1356, 814; MS (EI) 355, 278(b), 262, 235, 138. Anal. Calcd for C$_{24}$H$_{25}$N$_3$: C, 81.09; H, 7.08; N, 11.82. Found: C, 80.95; H, 7.05; N, 11.73; mp = 180−181 °C.

1,1,1-Tris(4-*N,N*-dimethylaminophenyl)ethane (1a)[88] (92% yield): ^{1}H NMR (200 MHz, CDCl$_3$) δ 6.98 (d, J = 8.8 Hz, 6H), 6.65 (d, J = 8.8 Hz, 6H), 2.91 (s, 18H), 2.08 (s, 3H); ^{13}C NMR (APT, 50 MHz, CDCl$_3$) δ 148.3, 138.5, 129.2, 111.9, 49.9, 40.6, 30.4; MS (EI) 387, 372(b), 356, 267, 186, 177, 171, 146, 141; mp = 210−212 °C.

1,1,1-Tris(4-*N,N*-dimethylaminophenyl)-2-phenyl-ethane (1b)[88] (89% yield): ^{1}H NMR (200 MHz, C$_6$D$_6$) δ 7.36 (d, J = 9.2 Hz, 6H), 7.08−6.94 (m, 5H), 6.56 (d, J = 9.2 Hz, 6H), 4.06, (s, 2H), 2.51 (s, 18H); MS (EI) 463, 372(b), 356, 186, 178, 91; mp = 182−183 °C.

Tris(4-aminophenyl)acetonitrile[22] (95% yield): ^{1}H NMR (200 MHz, CD$_3$CN) δ 6.85 (d, J = 8.8 Hz, 6H), 6.59 (d, J = 8.8 Hz, 6H), 4.23 (s, 6H); ^{13}C NMR (APT, 50 MHz, CD$_3$CN) δ 148.3, 129.0, 128.3, 124.9(CN), 113.7, 54.9; IR (KBr) cm^{-1} 3477, 3384, 2235(CN), 1629, 1511, 1302, 1180, 831; MS (EI) 314, 222(b), 205, 195, 184, 157; mp = 320−322 °C.

Triphenylacetonitrile (1t)[47] (89% yield): ^{1}H NMR (200 MHz, CDCl$_3$) δ 7.41−7.27 (m, 9H), 7.27−7.16 (m, 6H); ^{13}C NMR (APT, 50 MHz, CDCl$_3$) δ 140.1, 128.8, 128.6, 128.1, 123.4(CN), 57.3; MS (EI) 269, 192, 165(b), 115, 77, 51, 39; mp = 125−126 °C.

3-(4′-*N,N*-Dimethylaminobenzoyl)-*N,N,N,N*-tetramethylbenzidine (9): for X-ray crystallography structure report, see ref 54; ^{1}H NMR (400 MHz, CDCl$_3$:CD$_3$COCD$_3$ = 1:5, COSY agrees excellent with assignment) δ 7.73 (d, J = 9.2 Hz, 2H), 7.57 (dd, J_1 = 8.8 Hz, J_2 = 2.4 Hz, 1H), 7.44 (d, J = 8.8 Hz, 2H), 7.38 (d, J = 2.8 Hz, 1H), 7.06 (d, J = 8.8 Hz, 1H), 6.77 (d, J = 8.8 Hz, 2H),), 6.69 (d, J = 9.2 Hz, 2H), 3.07 (s, 6H), 2.95 (s, 6H), 2.71 (s, 6H); ^{13}C NMR (APT, DEPT, and ^{13}C, 50 MHz, CDCl$_3$) δ 196.6, 153.1, 149.3, 149.2, 132.3, 131.6, 130.7, 128.3, 127.7, 127.3, 126.8, 124.8, 116.6, 112.6, 110.2, 43.3, 40.4, 39.8; IR (KBr) cm^{-1} 2883, 2069, 1609, 1603, 1591, 1496, 1189, 809; MS (EI) 387, 370(b), 355, 326, 185, 177, 148, 134. Anal. Calcd for C$_{25}$H$_{29}$N$_3$O: C, 77.48; H, 7.54; N, 10.84. Found: C, 77.14; H, 7.55; N, 10.76; mp = 168−169 °C (decomp); λ_{max}(CHCl$_3$) = 339, 248 nm.

3-[(4′-*N,N*-Dimethylamino)-α-cyanobenzyl]-*N,N,N,N*-tetramethylbenzidine (7): ^{1}H NMR (400 MHz, CDCl$_3$) δ 7.54 (d, J = 2.4 Hz, 1H), 7.46 (dd, J_1 = 8.4 Hz, J_2 = 2.4 Hz, 1H), 7.42 (d, J = 8.8 Hz, 2H), 7.26 (d, J = 8.4 Hz, 1H), 7.23 (d, J = 8.8 Hz, 2H), 6.76 (d, J = 8.8 Hz, 2H), 6.65 (d, J = 8.8 Hz, 2H), 5.91 (s, 1H), 2.96 (s, 6H), 2.90 (s, 6H), 2.65 (s, 6H); ^{13}C NMR (APT, DEPT, and ^{13}C, 50 MHz, CDCl$_3$) δ 150.2, 149.8, 138.1, 133.3, 128.334, 128.280, 127.5, 127.1, 126.7, 124.0(CN), 121.6, 121.4, 112.7, 112.6, 45.9, 40.533, 40.460, 35.4(CH); IR (KBr) cm^{-1} 2961, 2792, 2234(CN), 1612, 1522, 1493, 1355, 1262, 945, 812; MS (EI) 398, 383, 339, 262, 235, 191, 169, 134(b); mp = 70−75 °C; HRMS (EI) calcd for C$_{26}$H$_{30}$N$_4$ 398.2470, found 398.2469.

4-Cyano-4,6-bis-(4′-*N,N*-dimethylaminophenyl)-1-methyl-1,2-dihydro-3,1,4-benzoxazine (8): ^{1}H NMR (400 MHz, CDCl$_3$, COSY agrees excellent with assignment) δ 7.47 (dd, J_1 = 8.8 Hz, J_2 = 2.2 Hz, 1H), 7.42 (d, J = 9.2 Hz, 2H), 7.34 (d, J = 9.2 Hz, 2H), 7.13 (d, J = 2.2 Hz, 1H), 6.93 (d, J = 8.8 Hz, 1H), 6.73 (d, J = 9.0 Hz, 2H),), 6.66 (d, J = 9.2 Hz, 2H), 5.00 (d, J = 9.6 Hz, 1H), 4.68 (d, J = 9.6 Hz, 1H), 3.01 (s, 3H), 2.94 (s, 6H), 2.93 (s, 6H); ^{13}C NMR (APT, DEPT, [13]C 50 MHz, and HMQC 400 MHz are all consistent, CDCl$_3$) δ 150.9, 149.5,

143.3, 133.1, 128.3, 128.1, 127.2, 127.0, 125.9, 125.6, 123.3(CN), 119.8, 116.8, 112.6, 111.7, 79.4(CH$_2$), 78.0(C), 40.4, 40.1, 38.3; IR (KBr) cm^{-1} 2890, 2809, 2224(CN), 1613, 1508, 1360, 1325, 1197, 808; MS (EI, 25 and 70 eV) 412(b), 395, 381, 369(b), 291, 251, 184, 148, 134; MS (CI) 413, 412, 387, 386(b), 374, 373, 370(b), 369, 292, 253, 148. Anal. Calcd for C$_{26}$H$_{28}$N$_4$O: C, 75.69; H, 6.84; N, 13.58. Found: C, 74.98; H, 6.86; N, 13.20; λ_{max}(CHCl$_3$) = 310 nm, 280 nm; HRMS (EI) calcd for C$_{26}$H$_{28}$N$_4$O 412.2263, found 412.2266.

4-*N,N*-Dimethylaminobenzoyl cyanide (10):[89] ^{1}H NMR (200 MHz, CDCl$_3$) δ 7.95 (d, J = 9.2 Hz, 2H), 6.69 (d, J = 9.2 Hz, 2H), 3.17 (s, 6H); ^{13}C NMR (APT and ^{13}C, 50 MHz, CDCl$_3$) δ 164.4(CO), 155.5, 133.0, 121.7, 113.8, 111.2, 40.2; IR (KBr) cm^{-1} 2926, 2214(CN), 1645, 1605, 1544, 1390, 1293, 1200, 824; MS (EI) 174, 173(b), 148, 118, 77; mp = 170−171 °C.

5-[(4′′-*N,N*-Dimethylamino)-α-cyanobenzyl]-4-(4′-*N,N*-dimethylaminophenyl)pyrocatechol (14): for X-ray crystallography structure report, see ref 54; ^{1}H NMR (200 MHz, CD$_3$COCD$_3$) δ 8.12 (s, 2H), 7.11 (d, J = 8.8 Hz, 2H), 6.99 (d, J = 8.8 Hz, 2H), 6.84 (s, 1H), 6.78 (d, J = 8.8 Hz, 2H), 6.73 (s, 1H), 6.68 (d, J = 8.8 Hz, 2H), 5.21 (s, 1H), 2.96 (s, 6H), 2.90 (s, 6H); ^{13}C NMR (APT, DEPT, and ^{13}C, 50 MHz, CDCl$_3$) δ 150.9, 150.7, 145.5, 145.3, 134.8, 130.7, 128.7, 126.9, 125.3, 121.8, 117.9, 116.0, 113.3, 113.0, 40.5, 40.4, 38.2(CH); IR (KBr) cm^{-1} 3489, 3257, 2881, 2800, 2255, 1608, 1514, 1441, 1353, 1095, 820; MS (EI) 387(b), 265, 251, 194, 193, 171, 159, 122; mp = 247−248 °C (decomp.).

4,4′-Bis(*N,N*-dimethylamino)dicyanostilbene (15):[90] mixture of E and Z isomers; ^{1}H NMR (400 MHz, CDCl$_3$) δ 7.30 (d, J = 9.2 Hz, 4H), 6.56 (d, J = 9.2 Hz, 4H), 3.01 (s, 12H); ^{13}C NMR (APT, DEPT, and ^{13}C, 50 MHz, CDCl$_3$) δ 151.2, 130.5, 120.2, 118.544, 118.380, 111.4, 39.9; IR (KBr) cm^{-1} 2902, 2821, 2217, 2208, 1603, 1515, 1371, 1197, 818; MS (EI) 316(b), 315, 301, 286, 229, 157, 149. λ_{max}(MeCN), nm 474, 392, 336, 270, 200; mp = 293−294 °C.

Bis(4-*N,N*-dimethylaminophenyl)-(4-*N*-methyl-*N*-formylaminophenyl)acetonitrile (18): ^{1}H NMR (200 MHz, CDCl$_3$) δ 8.51 (s, 1H), 7.30 (d, J = 8.8 Hz, 2H), 7.12 (d, J = 8.8 Hz, 2H), 7.05 (d, J = 9.1 Hz, 4H), 6.66 (d, J = 9.1 Hz, 4H), 3.31 (s, 3H), 2.94 (s, 12H); ^{13}C NMR (APT, DEPT, and ^{13}C, 50 MHz, CDCl$_3$) δ 162.1(CHO), 149.8, 141.3, 139.8, 129.9, 129.2, 127.6, 123.8, 121.6, 111.9, 55.3, 40.2, 31.8(HCON-Me); IR (KBr) cm^{-1} 2888, 2804, 2233, 1679, 1608, 1519, 1357, 1112, 813; MS (EI) 412, 292, 278(b), 262, 251, 206, 190; mp = 167−169 °C (decomp.); HRMS (EI) calcd for C$_{26}$H$_{28}$N$_4$O 412.2263, found 412.2264.

Bis(4-*N,N*-dimethylaminophenyl)-(4-*N*-methylaminophenyl)acetonitrile (17): ^{1}H NMR (200 MHz, CDCl$_3$) δ 7.06 (d, J = 9.2 Hz, 4H), 7.02 (d, J = 9.0 Hz, 2H), 7.64 (d, J = 9.2 Hz, 4H), 6.52 (d, J = 9.0 Hz, 2H), 2.93 (s, 12H), 2.80 (s, 3H); ^{13}C NMR (APT, DEPT, and ^{13}C, 50 MHz, CDCl$_3$) δ 149.6, 148.5, 129.88, 129.52, 129.35, 129.03, 124.6, 111.90, 111.85, 55.1, 40.4, 30.6 (ArNH-Me); IR (KBr) cm^{-1} 3396, 2884, 2803, 2229, 1609, 1519, 1354, 1184, 817; MS (EI) 384(b), 340, 278, 264(b), 248, 219, 190; mp = 228−229 °C.

3-[1′-(4′′-*N,N*-Dimethylaminophenyl)-(2′-phenyl)ethenyl]-*N,N,N,N*-tetramethylbenzidine (9b): E and Z isomers were separated and had identical NMR spectra; ^{1}H NMR (200 MHz, C$_6$D$_6$) δ 7.78 (d, J = 2.2 Hz, 1H), 7.66 (dd, J_1 = 8.8 Hz, J_2 = 2.2 Hz, 1H), 7.49 (d, J = 9.0 Hz, 4H), 7.39−7.30 (m, 2H), 7.12−6.85 (m, 5H), 6.55 (d, J = 9.0 Hz, 2H), 6.54 (d, J = 9.0 Hz, 2H), 2.57 (s, 6H), 2.50 (s, 6H), 2.48 (s, 6H); ^{13}C NMR (APT, DEPT, and ^{13}C, 50 MHz, C$_6$D$_6$) δ 150.7, 150.3, 149.7, 143.2, 139.0, 134.6, 132.9, 131.5, 131.0, 129.7, 129.4, 128.24, 128.20, 126.6, 126.3, 124.8, 118.8, 113.4, 112.5, 42.9, 40.3, 40.1; one isomer: MS (EI) 461, 446, 370(b), 355, 326, 223, 185, 177, 162, 134, 91; the other isomer: MS (EI) 461, 446, 370, 355, 326, 223, 185, 177, 162, 134(b), 91; mp = 176−178 °C (decomp); HRMS (EI) calcd for C$_{32}$H$_{35}$N$_3$O 461.2831, found 461.2827.

α-Phenyl-(4-*N,N*-dimethylamino)acetophenone (10b):[91] ^{1}H NMR (200 MHz, CDCl$_3$) δ 7.93 (d, J = 9.2 Hz, 2H), 7.34−7.14 (m, 5H), 6.63 (d, J = 9.2 Hz, 2H), 4.18 (s, 2H), 3.03 (s, 6H); ^{13}C NMR (APT and ^{13}C, 50 MHz, CDCl$_3$) δ 195.7(CO), 153.3, 135.7, 130.8, 129.3, 128.5, 126.4, 124.4, 110.6, 44.9(CH$_2$),

39.9; IR (KBr) cm^{-1} 2905, 2895, 1664(CO), 1602, 1376, 1189, 818, 720; MS (EI) 239, 148(b), 104, 91, 77; mp = 163−164 °C.

2-[1′′-(4′′′-*N,N*-Dimethylaminophenyl)-(2′′-phenyl)ethenyl]-4-(4′-*N,N*-dimethylaminophenyl)phenol (26b): ^{1}H NMR (200 MHz, CDCl$_3$) δ 7.49 (dd, J_1 = 8.8 Hz, J_2 = 2.2 Hz, 1H), 7.39 (d, J = 9.0 Hz, 2H), 7.31 (d, J = 9.0 Hz, 2H), 7.32 (d, J = 2.2 Hz, 1H), 7.23−7.12 (m, 6H), 6.97 (d, J = 8.8 Hz, 1H), 6.74 (d, J = 9.0 Hz, 2H), 6.67 (d, J = 9.0 Hz, 2H), 2.97 (s, 6H), 2.94 (s, 6H); ^{13}C NMR (APT, DEPT, and ^{13}C, 50 MHz, C$_6$D$_6$) δ 151.6, 150.4, 149.5, 136.8, 136.3, 133.9, 129.1, 128.9, 128.8, 128.7, 128.2, 128.0, 127.20, 127.16, 127.11, 126.6, 126.4, 116.0, 112.9, 112.2, 40.7, 40.4; IR (KBr) cm^{-1} 3430, 2895, 2800, 1604, 1521, 1355, 815; MS (EI) 434, 343, 312, 217, 216, 208, 171, 163, 134(b); HRMS (EI) calcd for C$_{30}$H$_{30}$N$_2$O 434.2358, found 434.2349.

4-Benzyl-4,6-bis(4′-*N,N*-dimethylaminophenyl)-1-methyl-1,2-dihydro-3,1,4-benzoxazine (8b): ^{1}H NMR (200 MHz, CDCl$_3$) δ 7.47 (d, J = 9.0 Hz, 2H), 7.43 (d, J = 2.0 Hz, 1H), 7.39 (dd, J_1 = 8.8 Hz, J_2 = 2.0 Hz, 1H), 7.36 (d, J = 8.8 Hz, 2H), 7.15−6.94 (m, 5), 6.81 (d, J = 9.0 Hz, 2H),), 6.79 (d, J = 8.8 Hz, 1H), 6.67 (d, J = 8.8 Hz, 2H), 4.35 (d, J = 9.2 Hz, 1H), 4.25 (d, J = 9.2 Hz, 1H), 3.69 (d, J = 13.8 Hz, 1H), 3.38 (d, J = 13.6 Hz, 1H), 2.98 (s, 6H), 2.93 (s, 6H), 2.58 (s, 3H); ^{13}C NMR (APT, DEPT, and ^{13}C 50 MHz) CDCl$_3$ δ 149.6, 149.4, 145.2, 137.5, 133.2, 131.5, 131.2, 128.8, 127.2, 127.1, 127.0, 126.3, 125.8, 125.2, 118.0, 113.0, 111.7, 81.9[Ar$_2$(Bn)C−O-], 77.0(N−CH$_2$−O), 48.8(PhCH$_2$-), 40.8, 40.5, 39.3; MS (EI) 477, 434, 386, 193, 170, 134(b), 91; HRMS (EI) calcd for C$_{32}$H$_{35}$N$_3$O 477.2780, found 477.2771.

2-[(4′-*N,N*-Dimethylamino)-α-cyanobenzyl]-4-phenyl-*N,N*-dimethylaniline (7′): ^{1}H NMR (200 MHz, CDCl$_3$) δ 7.56−7.16 (m, 7H), 7.44 (dd, J_1 = 9.2 Hz, J_2 = 2.2 Hz, 1H), 7.28 (d, J = 9.2 Hz, 2H), 6.74 (d, J = 9.0 Hz, 2H), 6.01 (s, 1H), 2.93 (s, 6H), 2.64 (s, 6H); ^{13}C NMR (APT, DEPT, and ^{13}C, 50 MHz, CDCl$_3$) δ 150.2, 149.8, 138.3, 136.5, 132.8, 128.75, 128.74, 127.6, 127.5, 127.4, 126.99, 126.95, 121.9, 120.8, 112.6, 45.8, 40.4, 36.3(CH); MS (EI) 355(b), 340, 313, 310, 269, 178, 170, 156, 117, 91; HRMS (EI) calcd for C$_{24}$H$_{25}$N$_3$ 355.2048, found 355.2048.

3-(α-Cyanobenzyl)-*N,N,N,N*-tetramethylbenzidine (7′′): ^{1}H NMR (200 MHz, CDCl$_3$) δ 7.60 (d, J = 2.2 Hz, 1H), 7.56−7.16 (m, 9H), 6.65 (d, J = 8.8 Hz, 2H), 5.92 (s, 1H), 2.88 (s, 6H), 2.66 (s, 6H); ^{13}C NMR (APT, DEPT, and ^{13}C, 50 MHz, CDCl$_3$) δ 151.3, 149.8, 140.2, 137.8, 133.4, 128.6, 128.2, 127.5, 127.4, 127.1, 126.9, 123.7, 121.6, 121.3, 112.5, 45.7, 40.3, 35.4(CH); MS (EI) 355, 340, 296, 234, 192, 178, 170, 156, 134(b), 121, 91; HRMS (EI) calcd for C$_{24}$H$_{25}$N$_3$ 355.2048, found 355.2050.

Supporting Information Available: Tables S1−S3 (yields of minor products; photophysical parameters of electron acceptors; observations in SS photolysis), Schemes S1−S8 (trapping with EtSH; irradiation of **1** in CHCl$_3$, **1** and benzophenone, **1** and DCA, and **1t**; photochemistry of CV radical; valence tautomerism of **6** and **4**; α,α-elimination), Figures S1−S8 (UV−vis of **1** irradiated in different solvents; kinetics of ^{3}**1***, **2**, and **3**; quenching of **1*** by oxygen; dark reaction and thermal bleaching; ORTEP drawings of **1**, **9**, and **14**). This material is available free of charge via the Internet at http://pubs.acs.org.

JO000374A